

Enumeration and representation of spin space groups

Jun Ren^{1,†}, Xiaobing Chen^{1,†}, Yanzhou Zhu^{2,†}, Yutong Yu¹, Ao Zhang¹,

Jiayu Li¹, Yuntian Liu¹, Caiheng Li² and Qihang Liu^{1,3,4,*}

¹*Shenzhen Institute for Quantum Science and Engineering and Department of Physics,
Southern University of Science and Technology, Shenzhen 518055, China*

²*National Center for Applied Mathematics Shenzhen, and Department of Mathematics,
Southern University of Science and Technology, Shenzhen 518055, China*

³*Guangdong Provincial Key Laboratory of Computational Science and Material
Design, Southern University of Science and Technology, Shenzhen 518055, China*

⁴*Shenzhen Key Laboratory of Advanced Quantum Functional Materials and Devices,
Southern University of Science and Technology, Shenzhen 518055, China*

[†]These authors contributed equally to this work.

*Email: liugh@sustech.edu.cn

Abstract

Those fundamental physical properties, such as phase transitions, Weyl fermions and spin excitation, in all magnetic ordered materials was ultimately believed to rely on the symmetry theory of magnetic space groups. Recently, it has come to light that a more comprehensive group, known as the spin space group (SSG), which combines separate spin and spatial operations, is necessary to fully characterize the geometry and underlying properties of magnetic ordered materials such as altermagnets. However, the basic theory of SSG has been seldomly developed. In this work, we present a systematic study of the enumeration and the representation theory of SSG. Starting from the 230 crystallographic space groups and finite translational groups with a maximum order of 8, we establish an extensive collection of over 100000 SSGs under a four-segment nomenclature. We then identify inequivalent SSGs specifically applicable to collinear, coplanar, and noncoplanar magnetic configurations. Moreover, we derive the irreducible co-representations of the little group in momentum space within the SSG framework. Finally, we illustrate the SSG symmetries and physical effects beyond the framework of magnetic space groups through several representative material examples, including a well-known altermagnet RuO_2 , spiral spin polarization in coplanar antiferromagnet CeAuAl_3 , and geometric Hall effect in noncoplanar antiferromagnet CoNb_3S_6 . Our work advances the field of group theory in describing magnetic ordered materials, opening up avenues for deeper comprehension and further exploration of emergent phenomena in magnetic materials.

I. Introduction

Symmetry has always been one of the core aspects of physics and material science. The crystallographic group theory, which was refined by Fedorov and Schönflies in the end of 19th century, provides a fundamental framework for understanding and predicting the properties and behavior of crystalline materials, facilitating advancements in fields ranging from solid-state physics and chemistry to materials engineering and drug discovery [1]. The complete set of symmetry elements exhibited by three-dimensional (3D) nonmagnetic or paramagnetic solids are depicted by 32 point groups (PGs) and 230 space groups (SGs), the latter of which include rotations, reflections, inversions, translations, and their combinations. The wavefunction properties of such crystals, like phase transition, selection rules and band degeneracy, are successfully described by the representations (reps) of 230 SGs.

The theory of crystalline group theory is further explored in the early 20th century, when Shubnikov and others realized that magnetic materials exhibit additional symmetries beyond the purely geometric symmetries found in nonmagnetic crystals. These additional symmetries arise from the magnetic moments associated with the atoms or ions within the crystal lattice. By introducing antiunitary time-reversal operation T that flips the direction of spin, the 32 PGs and 230 SGs are extended to 122 magnetic point groups (MPGs) and 1651 magnetic space groups (MSGs), respectively. With the development of X-ray diffraction and neutron diffraction techniques, the structure of a given magnetic crystal and the orientation of its spins can be determined and assigned a specific MSG. Since then, the theory of MSGs was believed as the ultimate theory in understanding the exotic properties such as ordering phenomena, phase transitions, spin excitation and band topology in all magnetic ordered materials [2-8].

However, as an axial vector, spin symmetry contains not only T that reverses its direction (like an inversion operator in spin space), but also spin rotation operations. The underlying concept of MPG and MSG is based on the assumption that a rotation operator acts simultaneously on spatial coordinate and spin coordinate. Exemplified by a simple collinear antiferromagnetic (AFM) order shown in Fig. 1, the system does not

exhibit any four-fold rotations within the regime of magnetic groups. However, if we consider the spatial coordinate and spin coordinate separately, the system thus has a spatial four-fold operation followed by a two-fold spin rotation. Therefore, from a geometric perspective, separating rotational operations from real space and spin space is necessary to fully describe the symmetry of a system with a vector field. Such an enhanced magnetic group, first proposed in the 1960s, is referred to as a spin group [9-13], which includes both spin point groups (SPGs) and spin space groups (SSGs).

From a physical perspective, spin group also constitutes the operator group of magnetic Hamiltonians, capturing the behavior of corresponding quasiparticles. Examples include single-particle Hamiltonians for electrons and the Heisenberg Hamiltonian for spin waves when spin-orbit coupling (SOC) is not considered [9,13,14]. Even in the presence of SOC with certain forms, the system can also manifest some hidden symmetries associated with a particular spin group [15-17]. With the recent prosperity of antiferromagnetic spintronics [18-20], it has been recognized that AFM order can generate various spintronics effects that are typically consequences for SOC, such as spin splitting, spin current and spin torque [21-39]. Consequently, spin group symmetries naturally serve as a starting point for investigating these Hamiltonians and related effects. For example, the recently discovered “altermagnetic phase” in collinear antiferromagnets, in which not only the magnetic moments are alternatively distributed in real space, but also the double-valued spin polarization alternatively distributed in momentum space, is defined in the SOC-free limit, and thus is delimited by spin groups [29,30]. Besides, spin group also helps to understand the band structures, topology, and transport phenomena in systems with negligible SOC [40-43], and provides descriptions about complex magnetic orderings (e.g., helical, spiral) [44].

The development of crystallographic group theory includes the enumeration and classification of groups, as well as the rep theory. While the theories of crystallographic groups and magnetic groups have been firmly established in textbooks [1,45], the theory of spin groups is still in its nascent stage, with only the enumeration of 598 SPGs completed by far [12]. The enumeration of SSGs and the relative rep theory describing wavefunction properties is still lacking. This is because the inclusion of degrees of

freedom in both real space and spin space poses significant challenges in the classification of SSGs. For example, the infiniteness of translation group implies an infinite number of SSGs. In this work, we present a systematic study of the enumeration and the rep theory of SSGs. The entire enumeration procedure starts from the 230 SGs, combining a translational supercell having a maximum order of 8. We traverse all inequivalent normal subgroups and establish their mapping onto a PG in spin space through inequivalent isomorphism relationships. Consequently, by means of group extension, we establish an extensive set of over 100000 SSGs. We then distinguish inequivalent SSGs for collinear, coplanar, and noncoplanar magnetic configurations, for which the nontrivial operations within spin space play a crucial role. In addition, we derive the irreducible co-reps of the little group at high-symmetry momenta within the framework of SSG. Finally, we provide several representative material examples, including an altermagnet RuO₂, a spiral antiferromagnet CeAuAl₃, and a noncoplanar antiferromagnet CoNb₃S₆ to demonstrate their SSG symmetries and physical properties beyond the framework of MSG, including the extra band degeneracies, spiral spin polarization and geometric Hall effect.

II. Enumeration of spin space groups

A. Methodology and nontrivial SSGs

Compared with conventional (magnetic) SGs, the key character of SSGs is that the spatial operations and spin operations are separately considered [9-13]. Therefore, the symmetry elements of spin groups can be written as $\{g_s||g_l\}$, where g_l denotes the spatial operation $\{C_n(\theta), IC_n(\theta)|\tau\}$ of the lattice ($C_n(\theta)$, I , and τ are the rotation of θ angle along \mathbf{n} axes, inversion and translation, respectively). To the left of the double bar, $g_s = \{U_m(\phi), TU_m(\phi)\}$ consists of spin rotations $U_m(\phi) \in SU(2)$ and the anti-unitary time-reversal operator T that reverses spin and momentum simultaneously. Similar to that of SPGs, the general form of SSGs, i.e., G_{SS} , could be expressed as the direct product of a nontrivial SSG G_{NS} and a spin-only group G_{SO} [11]:

$$G_{SS} = G_{NS} \times G_{SO}, \quad (1)$$

where G_{SO} only contains spin operations $\{g_s||E|0\}$; G_{NS} contains no pure spin

operations [11]. While for noncoplanar magnetic order $G_{SO}^n = \{E || E | 0\}$ (identity group), for coplanar magnetic order $G_{SO}^p = \{E, TU_n(\pi)\} = Z_2^K$, implying the mirror symmetry in spin space (\mathbf{n} is perpendicular to the coplanar order). For collinear magnetic order, $G_{SO}^l = Z_2^K \rtimes SO(2)$, where $SO(2) = \{U_z(\phi), \phi \in [0, 2\pi]\}$ contains full spin rotations along a specific axis z [13]. Next, we focus on the construction of nontrivial SSGs.

In analogy to the construction of 598 SPGs, the central idea of constructing nontrivial SSGs is based on the decomposition of normal subgroups of crystallographic SGs and group extension. First, a SG G_0 can be decomposed into cosets with respect to one of its normal subgroups L_0 ,

$$G_0 = L_0 \cup g_1 L_0 \cup \dots \cup g_{n-1} L_0. \quad (2)$$

When the resulting quotient group G_0/L_0 is isomorphic to a PG, one can use such a PG as the operations for spin space, $G^s = \{E, g_{s_1}, \dots, g_{s_{n-1}}\}$ ($g_{s_i} \in SO(3) \times \{E, T\} \cong O(3)$), and map G^s to G_0/L_0 through isomorphism relationship, forming a SSG written as

$$G_{NS} = L_0 \cup \{g_{s_1} || g_1\} L_0 \cup \dots \cup \{g_{s_{n-1}} || g_{n-1}\} L_0. \quad (3)$$

The enumeration of all the possible SSGs includes the exhaustively enumerating all (G_0, L_0) pairs and inequivalent choices of coset representative elements, listing all G^s isomorphic to G_0/L_0 in spin space, and finding all inequivalent mappings between G^s and G_0/L_0 . However, compared with that of SPGs, the enumeration of SSGs faces more challenges due to the existence of crystallographic translation groups of SGs. To distinguish difference cases, three types of subgroups L_0 are categorized:

1) A subgroup L_0 of a SG G_0 is referred to as a translationengleiche subgroup [46] or a t-subgroup of G_0 if their translation subgroup $T(G_0)$ is retained, i.e. $T(L_0) = T(G_0)$, while the PG part $P(L_0)$ is a subgroup, i.e., $P(L_0) < P(G_0)$. A SSG formed in this way is called a **t-type** SSG, in which the t-index i_t is used to present the reduction of the PG symmetry $i_t = |P(G_0)|/|P(L_0)|$. It is straightforward that the quotient groups G_0/L_0 of t-type SSGs must be isomorphic to one of the 32 crystallographic PGs.

Therefore, the derivation of 598 nontrivial SPGs can be directly extended to obtain t-type SSGs.

2) A subgroup L_0 of a space group G_0 is referred to as a klassengleiche subgroup [46] or a k-subgroup of G_0 if the PG part $P(G_0)$ is retained, i.e. $P(L_0) = P(G_0)$, while the translation subgroup $T(L_0)$ is reduced to $T(L_0) < T(G_0)$. A SSG formed in this way is called a **k-type** SSG, in which the k-index i_k is used to present the reduction of the PG symmetry $i_k = |T(G_0)|/|T(L_0)|$. In general, k-subgroup implies cell multiplication to accommodate the magnetic configuration. Therefore, unlike i_t that can be solely determined by the PG part of G_0 and L_0 , i_k is an independent condition to label an SSG. Importantly, the quotient group G_0/L_0 for a k-subgroup L_0 is Abelian with the form $Z_{n_1} \times Z_{n_2} \times Z_{n_3}$. As a result, the group structures of G_0/L_0 are not limited to 32 crystallographic PGs (could even be a non-PG) and are countless, leading to infinite numbers of SSGs. In this work, we set a cutoff of $i_k = n_1 n_2 n_3 \leq 8$ to enumerate the typical k-type SSGs. For example, the SSGs, whose translation quotient group G_0/L_0 has the structure of Z_5 , allow for a five-fold rotation of spins propagating along a specific direction. For the commensurate magnets with $i_k > 8$, their SSGs can still be diagnosed case by case by our procedure.

3) Those L_0 that have lost PG operations as well as translation operations are called general subgroups of G_0 [$P(L_0) < P(G_0)$ and $T(L_0) < T(G_0)$]. A SSG formed in this way is called a **g-type** SSG. Through the construction procedure, we find that g-type subgroups constitute most of the total (over 85%).

To mathematically enumerate all group-normal subgroup pairs (G_0, L_0) with a specific i_k index, we adopt an inverse procedure, starting from L_0 and finding all supergroups G_0 whose subgroup contain L_0 . The full list of group-normal subgroup pairs is obtained with the assistance of SUPERGROUPS program [47] implemented in Bilbao Crystallographic Server [48]. Then we exert the condition that L_0 is a normal subgroup of G_0 , leading to 10660 combinations of (G_0, L_0, i_k) . For each combination, there may be multiple possibilities with different coset representative elements, which relates to the symmetry operation between different magnetic sublattices. Furthermore,

for a given i_k there are also multiple possibilities fulfilling $i_k = n_1 n_2 n_3$, which correlates the cell expansion along different directions. Therefore, we utilize the chirality-preserving affine normalizer $N_{A^+}(L_0)$ to find all inequivalent coset decompositions [49]. All affine mappings [50] in \mathbb{R}^3 that map L_0 onto itself by conjugation and preserve its chirality form the chirality-preserving affine normalizer of L_0 :

$$N_{A^+}(L_0) = \{a | a^{-1} L_0 a = L_0, a \in \mathbb{R}^3 \rtimes SL(3, \mathbb{Z})\}. \quad (4)$$

Two pairs (G_0, L_0) and (G'_0, L_0) are equivalent if their supergroups are conjugated under $a \in N_{A^+}(L_0)$:

$$a^{-1} G'_0 a = G_0, \quad \exists a \in N_{A^+}(L_0) \quad (5)$$

After coset decomposition, we next consider the coupled symmetry group in spin space, $G^S \cong G_0/L_0$. The isomorphism implies that given a specific combination of (G_0, L_0, i_k) , G^S could have different PG forms. For example, if the quotient group G_0/L_0 is isomorphic to a D_8 , G^S could be D_8 , C_{8v} and D_{4d} . Moreover, for a given G^S , the isomorphic mapping between G^S and G_0/L_0 also have multiple possibilities, leading to different nontrivial SSGs according to Eq. (3). Two nontrivial SSG G'_{NS} and G_{NS} are equivalent if they can be mapped onto each other by:

$$a^{-1} G'_{NS} a = G_{NS}, \quad \exists a \in (N_{A^+}(L_0) \cap N_{A^+}(G_0)) \times N_{O(3)}(G^S), \quad (6)$$

where $N_{A^+}(G_0)$ is the chirality-preserving affine normalizer of G_0 and $N_{O(3)}(G^S)$ is the normalizer of G^S in orthogonal group $O(3)$. Finally, a SSG identified by a four-segment (G_0, L_0, i_k, m) label is constructed, with the last index m containing inequivalent coset decompositions of G_0/L_0 , different G^S and inequivalent mappings between G^S and G_0/L_0 . The mathematical procedure is done by using MAGMA [51].

Through the abovementioned methodology, we can mathematically obtain 122 types of G^S , and 100612 nontrivial SSGs (G_{NS}) with the cell expansion limited to $i_k \leq 8$. The full list, provided in Supplementary Materials, includes 8505 t-type, 6738 k-type and 85369 g-type SSGs. In Table I we show the number of SSGs classified by the crystal systems of G_0 , which is the SG of the nonmagnetic symmetry of the magnetic primitive cell. It is shown that the majority of the SSGs concentrates in crystal systems with

relatively lower symmetry, i.e., monoclinic, orthorhombic, and tetragonal (89% in total). We next take a series of t-type nontrivial SSGs to illustrate the correspondence of the group construction and the realistic magnetic structure. For clarity we use International symbol to present group operations hereafter, where I and T are denoted by $\bar{1}$ in real space and spin space, respectively. Considering two SGs $L_0 = P2/c$ (No. 13) and $G_0 = Pcca$ (No. 54) fulfilling normal subgroup relationship, $G_0 = L_0 \cup \{2_{010}|0,0,1/2\}L_0$. One can define two different sublattices [marked by different colors in Fig. 2(a)] with the group generators of L_0 keeping the sublattice invariant. Thus, L_0 can be defined as the sublattice group. On the other hand, the coset group elements of G_0 transform one sublattice to the other, as shown in Fig. 2(b). Therefore, there are three possibilities of G^S being isomorphic to G_0/L_0 i.e., $\bar{1}$, 2, and m , leading to three different mappings for the magnetic moments, as shown in Figs. 2(c-e). Taking (13.54.1.1) as an example, the nontrivial SSG is constructed by mapping the $\bar{1}$ operator in spin space (i.e., T) to the representative element $\{2_{010}|0,0,1/2\}$, leading to $G_{NS} = L_0 \cup \{\bar{1}|\{2_{010}|0,0,1/2\}L_0$. We develop a program to provide a convenient way to identify the SSG from a given magnetic structure. The detailed algorithm is described in Appendix A.

While there is no multiplicity of different mappings for a specific order-2 G^S , there is another inequivalent coset representative element $\{2_{001}|1/2,0,0\}$ for (L_0, G_0) , owing to the inequivalence between a and c axis for SG $P2/c$. Consequently, there are another three nontrivial SSGs with a different choice of sublattices, as shown in Figs. 2(f-h). Overall, there are 6 t-type nontrivial SSGs for the given (L_0, G_0) pair [Fig. 2(i)], with two supporting collinear magnetic structures ($G^S = \bar{1}$), and four of them supporting coplanar magnetic structures ($G^S = 2$ and m). However, we will show later that when considering spin-only group, the SSGs generated by $G^S = 2$ and m are indeed equivalent.

B. Inequivalent SSGs for different magnetic configurations

Table I also enumerate the nontrivial SSGs supporting collinear only, noncoplanar only, and coplanar magnetic configurations. We next implement spin-only group G_{SO} into G_{NS} to count all inequivalent SSGs for different magnetic configurations, including

collinear, coplanar and noncoplanar orders. We will elucidate that G_{SO} plays a crucial role in finding equivalent collinear and coplanar SSGs. Without the loss of generality, we assume that each sublattice only contains one type of magnetic ions. The enumeration process is based on different G^S , and is divided into the following steps:

1) Collinear SSGs. In collinear magnets, all local moments point towards the same or opposite direction (e.g., the z axis), and the corresponding SSG does not depend on the direction of the spins. The full SSG of a collinear magnet is written as $G_{SS} = G_{NS} \times Z_2^K \ltimes SO(2)$. The spin-only group $G_{SO}^l = Z_2^K \ltimes SO(2)$ of collinear SSG ensures that only time-reversal T needs to be considered for the spin space of G_{NS} , rendering only two possibilities, $G^S = 1$ and $\bar{1}$ corresponding to ferromagnets (ferrimagnets) and antiferromagnets, respectively. Therefore, collinear SSGs manifest one-by-one correspondence with the structure of MSGs, in which the magnetic sublattices with opposite directions of local moments can be regarded as black and white.

Specifically, there are 230 SSGs for collinear ferromagnets or ferrimagnets with their nontrivial SSG $G_{NS} = G_0$, where G_0 is one of the 230 SGs. These nontrivial t-type SSGs also have $G_0 = L_0$, corresponding to 230 type-I MSGs. For antiferromagnets, the nontrivial SSG can be written as $G_{NS} = L_0 \cup \{T|A\}L_0$, where A denotes the symmetry operation connecting the sublattices with opposite spins. If A is a pure translation, i.e., $P(L_0) = P(G_0)$ and $i_k = 2$, the resulting SSGs correspond to 517 type-IV MSGs. On the other hand, if A is inversion or rotation (proper or improper), the resulting SSGs with $T(L_0) = T(G_0)$ and $i_t = 2$ correspond to 674 type-III MSGs. Overall, there are 1421 inequivalent collinear SSGs in total, as marked by double star in Supplementary Materials.

2) Coplanar SSGs. For those SSGs describing coplanar magnetic configurations, the spin-only group is $G_{SO}^p = \{E, TU_n(\pi)\}$. Thus, all the spin rotation axes of G^S should be either perpendicular or parallel to a specific axis \mathbf{n} , implying that polyhedral PGs are excluded for G^S . In addition, due to the existence of the spin-only group G_{SO}^p , we can further limit G^S to unitary PGs, which do not contain T . To prove this, we consider an antiunitary nontrivial SSG G_{NS}^{AU} with its maximal unitary subgroup L^{MU} :

$$\begin{aligned}
G_{NS}^{AU} \times \{E, TU_n(\pi)\} &= [L^{MU} \cup (G_{NS}^{AU} \setminus L^{MU})] \times \{E, TU_n(\pi)\} \\
&= [L^{MU} \cup TU_n(\pi)(G_{NS}^{AU} \setminus L^{MU})] \times \{E, TU_n(\pi)\} = G_{NS}^U \times \{E, TU_n(\pi)\}. \quad (7)
\end{aligned}$$

Eq. (7) suggests the equivalence between antiunitary SSG G_{NS}^{AU} and unitary SSG G_{NS}^U when taking G_{SO}^p into account. Therefore, to obtain all coplanar SSGs from the full (G_0, L_0, i_k, m) SSG list, it is adequate to add the condition $G^S \cong C_n$ or D_n . Note that for k -subgroups and g -subgroups, C_n and D_n groups are not limited to be crystallographic PGs (e.g., Z_5), resulting in 40 possibilities in total. Within considered cell multiplicity $i_k \leq 8$, we find 16383 inequivalent coplanar SSGs, which is significantly reduced compared with the number of G_{NS} that support coplanar magnetic configurations.

We note two special portions of G_{NS} for coplanar configurations. The first one is $G^S = 2$ and m , for which the G_{NS} support both collinear and coplanar (but not noncoplanar) configurations. However, when they describe collinear configurations, they are exactly equivalent to the SSGs with $G^S = \bar{1}$ due to the existence of G_{SO}^l , so they do not contribute new entries to 1421 inequivalent collinear SSGs. On the other hand, when they describe coplanar configurations, they are equivalent to each other because of Eq. (7), contributing 1191 inequivalent coplanar SSGs. Therefore, there are 1191 entries with $G^S = m$ rendering equivalent SSGs when considering G_{SO} part. Specifically, as for our example, (13.54.1.2) and (13.54.1.3) [Figs. 2(b) and 2(c)] are equivalent coplanar SSGs.

The second case is $G^S = 2/m$, for which the G_{NS} support coplanar configurations only. However, considering G_{SO}^p , the SSGs generated by antiunitary $2/m$ is equivalent to those generated from $G^S = 222$ according to Eq. (7). Therefore, there are 9501 entries with $G^S = 2/m$ rendering equivalent SSGs when considering G_{SO} part.

3) Noncoplanar SSGs. The spin-only group for noncoplanar SSGs is simply identity group. When G^S is a polyhedral PG (T , T_d , T_h , O , and O_h), there are 357 SSGs in total supporting only noncoplanar magnetic configurations. On the other hand, when taking other G^S except 1 , $\bar{1}$, 2 , m , $2/m$, and polyhedral PGs, the corresponding G_{NS} (86951 entries) support both coplanar and noncoplanar configurations. Since $G_{SS} = G_{NS}$, all these SSGs for noncoplanar configurations are inequivalent. Finally,

there are 87308 inequivalent noncoplanar SSGs in total.

We show in Fig. 3 the summary of the inequivalent SSGs for different magnetic configurations, indicating that the spin-only groups serve as another factor for equivalent SSGs. For example, the nontrivial SSGs supporting coplanar magnetic configurations indeed form a small subset for inequivalent coplanar SSGs.

III. Representation of spin space groups

Representation theory is the key to encode the information of symmetry to quantum-mechanics wavefunctions, which determine the elementary excitations, geometric phases, selection rules, etc. While there exists symmetry arguments for band degeneracy within the regime of SSGs [44], a systematic survey of the rep theory of SSGs, especially the irreducible co-reps (co-irreps) of the little group at high-symmetry momenta, is still lacking. We next explore the general rep theory of SSGs. We will separately consider the SSGs supporting noncollinear (coplanar and noncoplanar) and collinear magnetic configurations, because the latter possesses infinite symmetry operations owing to the spin-only group $Z_2^K \ltimes SO(2)$.

A. Coplanar and noncoplanar SSGs

To obtain the irreps and co-irreps of SGs and MSGs, the typical approach involves the identification of the abstract group isomorphic to the little group of k , and central extension for nonsymmorphic groups [45]. However, SSGs contain some “spin nonsymmorphic symmetries”, i.e., combined operations of spin rotation and translation, that keep k invariant. As a result, the little group and the corresponding abstract group could be very complicated. Instead, we examine the regular projective reps of SSGs, in which both spin rotations and translations are integrated into the phase factor. We then apply an approach that utilizes the eigenvalues and eigenvectors of a complete set of commuting operators (CSCO) to obtain all irreps of unitary SSGs [52,53]. Finally, we demonstrate that Dimmock and Wheeler’s character sum rule can be extended to projective reps, to derive the co-irreps of anti-unitary SSGs.

In SGs, a projective irrep $M_k^l(\{R_i|\tau_i\})$ of a little group of wavevector k leaves the complexity of fractional translation from nonsymmorphic operations to the phase factor, i.e., $d_k^l(\{R_i|\tau_i\}) = \exp(-ik \cdot \tau_i) M_k^l(\{R_i|\tau_i\})$, where $d_k^l(\{R_i|\tau_i\})$, R_i and τ_i denote the l -th irrep of the little group, inversion, rotations or rotoinversions in lattice space, and translation. The phase factor can also absorb the additional phase of spin rotation $U_m(\phi)$, where each rotation of 2π picks up a phase of -1. Unlike SGs, a single lattice operation R_i in SSGs may correspond to multiple nonsymmorphic translations τ_i^a for the case of $i_k > 1$, as well as spin operations $g_{s_i}^a$. Considering $d_k^l(\{g_{s_i}^a||R_i|\tau_i^a\})$ an irrep of a unitary little SSG G_{SS}^k , we have:

$$d_k^l(\{g_{s_i}^a||R_i|\tau_i^a\}) = \pm \exp(-ik \cdot \tau_i^a) M_k^l(\{g_{s_i}^a||R_i|\tau_i^a\}). \quad (8)$$

Here “+” and “-” apply for $0 \leq \phi(g_{s_i}^a) < 2\pi \pmod{4\pi}$ and $2\pi \leq \phi(g_{s_i}^a) < 4\pi \pmod{4\pi}$, respectively, in which $\phi(g_{s_i}^a)$ is the rotation angle of $g_{s_i}^a$. We note that projective reps do not distinguish translations up to integer multiplications of lattice vectors, i.e., $M_k^l(\{g_{s_i}^a||R_i|\tau_i^a + t_i\}) = M_k^l(\{g_{s_i}^a||R_i|\tau_i^a + t_j\})$ for $t_i, t_j \in T(L_0)$. That is to say, $M_k^l(\{g_{s_i}^a||R_i|\tau_i^a\})$ is matrix-valued function on the elements $\{g_{s_i}^a||R_i|\tau_i^a\}$ of the finite quotient group $\tilde{G}_{SS}^k = G_{SS}^k/T(L_0)$ with the order $N_k = |\tilde{G}_{SS}^k|$. According to the multiplication of reps d_k^l , for the projective reps of elements $\{g_{s_i}^a||R_i|\tau_i^a\}$, $\{g_{s_j}^a||R_j|\tau_j^a\} \in \tilde{G}_{SS}^k$ [$0 \leq \phi(g_{s_i}^a), \phi(g_{s_j}^a) < 2\pi$] we have:

$$M_k^l(\{g_{s_i}^a||R_i|\tau_i^a\}) M_k^l(\{g_{s_j}^a||R_j|\tau_j^a\}) = (-1)^{\xi(\phi(g_{s_i}^a))} \exp(-iK_i \cdot \tau_j) M_k^l(\{g_{s_i}^a||R_i|\tau_i^a\}). \quad (9)$$

Here $\{g_{s_i}^a||R_i|\tau_i^a\} = \{g_{s_i}^a g_{s_j}^a||R_i R_j|(\tau_i^a + R_i \tau_j^a) \pmod{T(L_0)}\}$, $K_i = R_i^{-1}k - k$, $\xi(\phi(g_{s_i}^a)) = 0$ or 1 if $0 \leq \phi(g_{s_i}^a) < 2\pi$ or $2\pi \leq \phi(g_{s_i}^a) < 4\pi$, respectively. Therefore, it is only necessary to find out all projective irreps of \tilde{G}_{SS}^k . For simplicity, we use g_i^a to represent $\{g_{s_i}^a||R_i|\tau_i^a\}$ hereafter.

Next, we exploit the CSCO method to obtain projective irreps by decomposing the regular projective reps. In quantum mechanics, CSCO (J^2, J_z) is used to label a state

$|j, m_j\rangle$ when dealing with a spherical symmetric potential of atoms. The corresponding quantum numbers, j and m_j , are sufficient to label all the eigenstates of the Hamiltonian. Similarly, CSCO could also be used to decompose the projective reps of \tilde{G}_{SS}^k . The procedure is introduced in the following:

1) Left regular projective reps: we can construct left regular projective reps by using the group elements $g_i^a \in \tilde{G}_{SS}^k$ as bases $|g_i^a\rangle$. A group element g_i^a acts on $|g_j^a\rangle$ as:

$$g_i^a |g_j^a\rangle = (-1)^{\xi(\phi(g_{s_l}^a))} \exp(-iK_i \cdot \tau_j) |g_l^a\rangle. \quad (10)$$

The resulting projective rep $M_k(g_i^a)$ is a reducible matrix of $N_k \times N_k$ dimensions with matrix elements $M_k(g_i^a)_{g, g_j^a} = \langle g | g_i^a | g_j^a \rangle = (-1)^{\xi(\phi(g_{s_l}^a))} \exp(-iK_i \cdot \tau_j) \delta_{g, g_i^a g_j^a}$.

2) Intrinsic regular projective reps: each group element $g_i^a \in \tilde{G}_{SS}^k$ corresponds to an element \bar{g}_i^a in the intrinsic group $\overline{\tilde{G}_{SS}^k}$, which obey right multiplication rule with $\bar{g}_i^a g_j^a = g_j^a \bar{g}_i^a$. Distinct from the typical right regular reps, $\overline{\tilde{G}_{SS}^k}$ is anti-isomorphic to \tilde{G}_{SS}^k . Thus, one can define the intrinsic regular projective reps:

$$\bar{g}_i^a |g_j^a\rangle = (-1)^{\xi(\phi(g_{s_m}^a))} \exp(-iK_j \cdot \tau_i) |g_m^a\rangle, \quad (11)$$

in which $g_m^a = \{g_{s_m}^a | |R_m| \tau_m^a\} = \{g_{s_j}^a g_{s_i}^a | |R_j R_i| (\tau_j^a + R_j \tau_i^a)\}$.

We next block diagonalize the left regular projective reps $M_k(g_i^a)$ that contain all the projective irreps. First, we consider unitary \tilde{G}_{SS}^k , in which the character χ_i^l of a projective irrep is a function of class operators:

$$C_i^a = \sum_{g_j^a \in \tilde{G}_{SS}^k} M_k(g_j^a)^{-1} M_k(g_i^a) M_k(g_j^a). \quad (12)$$

The number of independent classes N_c is equal to the number of projective irreps; and a n_l -dimensional projective irreps will appear n_l times in $M_k(g_i^a)$. By constructing the linear combination of class operators $C = \sum_i k_i C_i^a$ (k_i are arbitrary constant numbers), we can decompose $M_k(g_i^a)$ into N_c blocks. Thus, N_c resembles the quantum number j in a quantum state $|j, m_j\rangle$.

The next quantum number is obtained from the canonical subgroup chain of \tilde{G}_{SS}^k , $\tilde{G}_{SS}^k(s) = \tilde{G}_{SS1}^k > \tilde{G}_{SS2}^k > \dots$ [53,54]. The collection of the corresponding class

operators $C(s) = (C(\tilde{G}_{SS1}^k), C(\tilde{G}_{SS2}^k), \dots)$ commute with the C , forming a CSCO set of $(C, C(s))$ together with C . Such a set helps us to distinguish the rows of a n_l -dimensional block of $M_k(g_i^a)$. However, in a left regular projective rep, an n_l -dimensional projective irrep occurs n_l times. Therefore, we need another canonical intrinsic subgroup chain, $\overline{\tilde{G}_{SS}^k}(s) = \overline{\tilde{G}_{SS1}^k} > \overline{\tilde{G}_{SS2}^k} > \dots$ and the corresponding class operators, $\bar{C}(s) = (\bar{C}(\tilde{G}_{SS1}^k), \bar{C}(\tilde{G}_{SS2}^k), \dots)$ would lift the remaining degeneracy. Finally, we have a CSCO set of $(C, C(s), \bar{C}(s))$ and a corresponding collection of eigenvalues, say $|j, m_j, \bar{m}_j\rangle$, of group \tilde{G}_{SS}^k . By rearranging their eigenvectors, we can construct a transformation matrix to block diagonalize $M_k(g_i^a)$ and get all projective irreps.

For antiunitary little SSG G_{SS}^k , one can always decompose it with respect to its maximal unitary subgroups L_{SS}^k : $G_{SS}^k = L_{SS}^k \cup TAL_{SS}^k$, where TA is the antiunitary coset representative element $\{T|A\}$. The projective irreps $M_k^l(g_i^a)$ and the corresponding irreps $d_k^l(g_i^a)$ for $g_i^a \in \tilde{L}_{SS}^k$ can certainly be treated by using the CSCO method discussed above. Assuming that the basis set of $d_k^l(g_i^a)$ is $|\psi\rangle = |\psi_1, \psi_2, \dots, \psi_{n_l}\rangle$, then for the coset the basis set can be adopted as $|\phi\rangle = |\phi_1, \phi_2, \dots, \phi_{n_l}\rangle = TA|\psi_1, \psi_2, \dots, \psi_{n_l}\rangle$. Consequently, the co-reps for the full basis set $|\psi, \phi\rangle$ are:

$$\begin{aligned} D_k^l(g_i^a) &= \begin{bmatrix} d_k^l(g_i^a) & 0 \\ 0 & d_k^l(A^{-1}g_i^aA)^* \end{bmatrix}, \\ D_k^l(TAg_i^a) &= \begin{bmatrix} 0 & d_k^l(TAg_i^aTA) \\ d_k^l(g_i^a)^* & 0 \end{bmatrix}. \end{aligned} \quad (13)$$

Then we can prove the following modified Dimmock and Wheeler's character sum rule, which helps to identify whether the co-reps are irreducible or not:

$$\sum_{g_i^a \in \tilde{L}_{SS}^k} \chi(d_k^l((TAg_i^a)^2)) = \begin{cases} +N_k & (a) \\ -N_k & (b) \\ 0 & (c) \end{cases}. \quad (14)$$

For case (a), the co-rep matrixes D_k^l in Eq. (13) are reducible and have the same dimension as the irrep d_k^l . For cases (b) and (c), the dimension of D_k^l is doubled compared with that of d_k^l . Following the approach presented here, we can obtain the projective co-irreps of an arbitrary k -point for all finite SSGs. The examples of these

co-reps and the resulting electronic band degeneracies for realistic materials are shown in Sec. IV.

B. Collinear SSGs

The CSCO method cannot be applied to collinear SSGs because the $SO(2)$ spin rotation symmetry renders the SSG an infinite group. Fortunately, thanks to the correspondence between collinear SSGs and 1421 MSGs (Type-I, III and IV), the co-reps of collinear SSGs can be obtained by considering the co-reps of MSGs plus the extra degeneracies originated from crucial spin symmetries, including spin $SO(2)$, $\{TU_n(\pi)\|E\}$ and $\{U_n(\pi)\|A\}$. Since $SO(2)$ group provides irreps labeled by double-valued spin angular momentum m_s (for both fermions and bosons), there are several degeneracy doubling mechanisms as follows: (i) the combination of $SO(2)$ with unitary $\{U_n(\pi)\|A\}$ symmetry pairs two conjugated one-dimensional (1D) irreps ($\pm m_s$) into a two-dimensional (2D) irrep. (ii) the combination of $SO(2)$ with antiunitary $\{T\|A\}$ pairs two conjugated 1D irreps into a 2D co-irrep. (iii) the antiunitary $\{TU_n(\pi)\|E\}$ can pair two conjugated irreps of real-space operations.

For 230 SSGs describing collinear ferromagnets or ferrimagnets, the nontrivial SSGs has the form $\{E\|G_0\}$ because $G^S = 1$. Due to the doubling mechanism (iii), the irreps have the same form as the single-valued irreps of type-II MSGs. For other SSGs describing collinear AFMs, the SSGs are written as $(L_0 \cup \{T\|A\}L_0) \times G_{SO}^l$. Therefore, the dimensions of the co-irreps remain the same as the single-valued irreps of type-II MSGs but irreps will be doubled if the k -points have the symmetry $\{U_n(\pi)\|A\}$ or $\{T\|A\}$.

IV. Realistic materials

While SOC ultimately exists in realistic magnetic systems, under the circumstances when SOC effect is weak or when considering the SOC-induced effects (e.g., orbital polarization) [55], it is useful to analyze the wavefunction properties of a SOC-free Hamiltonian [13]. SSGs provide a comprehensive symmetry description of such Hamiltonians. In the following, we perform density functional theory (DFT)

calculations (see Appendix B for DFT methods) on several material candidates to exemplify their spin group symmetries, the electronic band degeneracies, spin textures, geometric Hall effects and the distinctions from MSG. Importantly, we show that the spin space part and real space part of a SSG directly lead to the features of spin polarization and geometric Hall effect, respectively. Our representative examples include the prototypical altermagnet RuO_2 (t-type SSG), spiral antiferromagnet CeAuAl_3 (k-type SSG) with coplanar configuration, and noncoplanar antiferromagnet CoNb_3S_6 (g-type SSG).

A. Extra band degeneracies in altermagnet RuO_2

RuO_2 is an altermagnet with a spin-polarized Fermi surface, and thus holds great potential to realized various spintronic effect, including spin-polarized current, giant magnetoresistance and spin-splitting torque [31-39]. It has a rutile structure with an out-of-plane collinear AFM order, with Ru and O ions occupying 2a and 4f Wyckoff positions, respectively [Fig. 4(a)]. The resulting nonmagnetic SG and MSG is $P4_2/mnm$ (No. 136) and $P4_2'/mnm'$ (136.499), respectively. To elucidate its SSG, we first determine its sublattice SG L_0 by considering the little group of SG that preserves the moment of Ru, i.e., $L_0 = Cmmm$ (No. 65). It is a t-type normal subgroup of $G_0 = P4_2/mnm$, with the subgroup indices $i_t = 2$, $i_k = 1$. The coset representative element, which is the symmetry connecting the sublattices with opposite magnetic moments, is a nonsymmorphic four-fold rotation $\{4_{001}^1|1/2,1/2,1/2\}$, and the coupled spin-space PG is $G_s = \bar{1} = \{E, T\}$. Consequently, the nontrivial SSG has the form $G_{NS} = L_0 \cup \{\bar{1}||4_{001}^1|1/2,1/2,1/2\}L_0$, labeled as (65.136.1.1); the full SSG is written as $G_{SS} = G_{NS} \times Z_2^K \rtimes SO(2)$, which is an infinite group.

Fig. 4(c) shows the band structure of RuO_2 calculated by DFT. It can be found that the bands along several high-symmetry lines, such as Γ -X-M, Γ -Z-R-A, have two-fold band degeneracies, while significant spin splittings occur along Γ -M and A-Z. The dimensions of the projective co-irreps for these wavevectors are shown in Fig. 4(d), demonstrating that the rep theory successfully reproduces the calculated band degeneracies. In comparison, we also plot in Fig. 4(e) the band structure with SOC,

where the band degeneracy is dictated by the co-reps of MSG [Fig. 4(f)]. It is shown that the high-symmetric line Z-R-A manifest band splitting with SOC, consistent with the MSG co-irreps. While the little magnetic groups of k along Z-R-A ($mm2$ or mmm) only support 1D co-irreps, the little spin groups of these k -points have the operation $\{\bar{1}||m_{010}\}(\bar{1}m)$, which can stick two conjugate co-irreps of $SO(2)$ ($^\infty 1$) forming extra degeneracies. Similar extra degeneracies protected by SSG have also been discussed in CoNb_3S_6 with collinear order [42,43], and Mn_3Sn with coplanar magnetic order [13]. On the other hand, the little spin group $^1m^mm^1m^\infty 1$ at Σ and S points does not support 2D co-irreps, thus leading to spin splitting even without SOC.

B. Spiral spin polarization in helimagnet CeAuAl_3

Spiral magnets, or helimagnets, present a type of magnetic ordering where the neighboring magnetic moments arrange in a spiral pattern, with a characteristic turn angle between 0 and 180 degrees. In general, such magnetic orders are originated from the competition between FM and AFM exchange interactions. Spiral magnets usually manifest combined spin rotation and fractional translation symmetry operations, which are not allowed within in the framework of MSG. However, for commensurate magnetic configurations, they serve as a nice platform to illustrate k-type and g-type SSGs. CeAuAl_3 has a tetragonal crystal structure with in-plane coplanar AFM order [56], with magnetic Ce ion occupying 4a Wyckoff positions [Fig. 5(a)]. The spin of the Ce layer rotates $\pi/2$ when moving to its neighboring Ce layer, resulting a spiral configuration with a four-fold cell expansion. While its nonmagnetic SG is $I4mm$ (No. 107), the MSG is degraded to $Pc4_1$ (76.10), with only 4 symmetry operations left. Within the regime of SSG, its sublattice group is $L_0 = P4mm$ (No. 99), a k-type normal subgroup of $G_0 = I4mm$, with the subgroup indices $i_t = 1$, $i_k = 4$. The coset representative element connecting the neighboring sublattices (Ce layers) is a fractional translation $\{1|1/2,1/2,1/4\}$, and the coupled spin-space PG is $G_s = 4_{001}$. Consequently, the nontrivial SSG has the form $G_{NS} = L_0 \cup \{4_{001}^1||1|1/2,1/2,1/4\}L_0 \cup \{2_{001}||1|0,0,1/2\}L_0 \cup \{4_{001}^3||1|1/2,1/2,3/4\}L_0$, labeled as (99.107.4.1); the

full SSG is written as $G_{SS} = G_{NS} \times Z_2^K$, which has 64 symmetry operations. Specifically, it has a screw axis in spin space, i.e., $\{4_{001}^1 || 1|1/2, 1/2, 1/4\}$.

The DFT-calculated local moment for each Ce ion is $0.98 \mu_B$, which is close to the experimental value ($1.05 \mu_B$ [56]). Fig. 5(b) exhibits the DFT-calculated band structure of CeAuAl₃. We find that the all the bands along the X-M line are four-fold degenerate, and some of these bands split into two branches of doubly degenerate bands along the Γ -X line. For Γ and Z points, both Dirac and Weyl nodes exist. These node features are well explained by our CSCO projective rep theory, which is applicable for finite groups. The detailed co-irreps for different wavevectors are provided in Appendix C. As shown in Fig. 5(e), while X-M line only supports 4D co-irreps, Γ and Z points also allow 2D co-irreps. Importantly, while it is believed that the existence of “ $U\tau$ ” symmetry (here is $\{2_{001} || 1|0,0,1/2\}$) protects spin degeneracy throughout the Brillouin zone [26,57], in CeAuAl₃ there are also 1D co-irreps for the little co-groups along Γ -Z, indicating spin splitting. Our results also highlight the crucial role of $SO(2)$ spin rotation, i.e., in collinear magnets, to manifest $U\tau$ -enforced spin degeneracy throughout the whole Brillouin zone [42,43].

More remarkably, such spiral magnets exhibit a new type of spiral spin polarization, for which the spin component aligns the spiral axis, rather than the direction of local moments. Fig. 5(d) shows the spin texture of CeAuAl₃ at the $k_z = \pi/2$ plane for the band marked in Fig. 5(b). While all the local moments are in-plane, the S_x and S_y components is enforced to be zero, leaving significant and continuous S_z distribution along the spiral direction (k_z). Such spiral spin polarization is in sharp contrast to the conventional Rashba and Dresselhaus spin polarization (along the k -dependent effective magnetic field) in nonmagnetic materials and Zeeman spin polarization (along the direction of local moments) in FM materials. To explain this, we note that the spin-space PG for an arbitrary k -point is 4, indicating that the spin texture has only S_z component and forms a four-fold symmetric pattern, consistent with our calculation shown in Fig. 5(d). Therefore, while such spin polarization can survive with moderate SOC, its physical mechanism is apparently beyond the scenario of MSG.

C. Geometric Hall effect in nonplanar CoNb₃S₆

CoNb₃S₆ has attracted great interest due to its surprisingly large anomalous Hall effect and controversial magnetic configurations [43,58-62]. While its magnetic order was historically determined as collinear AFM by neutron diffraction measurements [63], recent study reported an all-in–all-out noncoplanar AFM order and accompanied topological Hall effect [62]. Here we discuss the SSG symmetry of CoNb₃S₆ with the all-in–all-out AFM order, and conclude that such a noncoplanar order generates anomalous Hall effect even without the assistance of SOC. As shown in Fig. 6(a), CoNb₃S₆ has a tetragonal crystal structure (nonmagnetic SG is No. 182, $P6_322$) with magnetic Co ion occupying 2d Wyckoff positions. Interestingly, its all-in–all-out AFM order forms a cubic structure in spin space, i.e., $G_s = \bar{4}3m$, resulting a combined SSG with real space and spin space coming from totally incompatible crystal systems. The corresponding SSG is g-type, labeled as (4.182.4.2), with the subgroup indices $i_t = 6$, $i_k = 4$. Since G_{SO} is the identity group, the full SSG has 48 symmetry operations. In contrast, the corresponding MSG is reduced to $P32'$ (6 elements) because within in such framework the spin rotation must compromise the spatial rotation, implying that the cubic nature of spin symmetry is lost.

The noncoplanar magnetic order could lead to responses without the assistance of SOC. For example, anomalous Hall effect has for long been attributed as a consequence of SOC under time-reversal breaking [64]. On the other hand, the exchange field induced by noncoplanar order could also induce anomalous Hall effect without SOC. Instead of topological Hall effect, we use the terminology of geometric Hall effect to emphasize the sole origin of magnetic geometry. While the characteristic quantities of noncoplanar magnets, e.g., scalar spin chirality [65] or band-resolved Berry curvature [66], cannot fully describe the existence of geometric Hall effect, we note that due to the absence of SOC, the geometric Hall conductivity tensor can be fully determined by SSG. For collinear and coplanar orders, the spin-only symmetry $TU_n(\pi)$ naturally forbids geometric Hall conductivity σ_{xy}^G . Therefore, the anomalous Hall effect in collinear or coplanar magnets (even for FM) must be a SOC effect. However, for

noncoplanar CoNb_3S_6 , the PG symmetry of real space part of the SSG is $62'2'$, which allows nonzero orbital magnetization along the z direction and thus σ_{xy}^G . The DFT-calculated geometric Hall conductivity is shown in Fig. 6(d), consistent with our symmetry analysis. Remarkably, σ_{xy}^G reaches $47 \text{ } \Omega^{-1}\text{cm}^{-1}$ at the Fermi level, which is comparable to the largest anomalous Hall conductivities in antiferromagnets with the assistance of SOC [67].

V. Summary

To conclude, we present a systematic study of the enumeration and the representation theory of SSG applied for describing different magnetic configurations. By using group extension approach, our enumeration constructs a collection of over 80000 nontrivial SSGs, named by a four-segment nomenclature. When considering spin-only operations for different magnetic configurations, we obtain 1421, 16383, and 87308 inequivalent collinear, coplanar, and noncoplanar SSGs, respectively. Furthermore, we derive the irreducible projective co-representations of the little groups of the wavevectors within the SSG framework, which is the foundation to understand the symmetry enforced degeneracies in band spectra. We then show representative material examples, including altermagnet RuO_2 , helimagnets CeAuAl_3 , and noncoplanar antiferromagnet CoNb_3S_6 to illustrate their SSG symmetries and the emergent properties beyond the MSG framework. Our work further develops the group theory in describing materials with magnetic order, thereby unlocking possibilities for future exploration into exotic phenomena within magnetic materials.

Note added. During the finalization of our work, we became aware of related studies on the classification of spin space groups from Chen Fang's and Zhi-Da Song's groups [68,69].

Acknowledgements

We thank Pengfei Liu for helpful discussions. This work was supported by National

Key R&D Program of China under Grant No. 2020YFA0308900, the National Natural Science Foundation of China under Grant No. 12274194, Guangdong Provincial Key Laboratory for Computational Science and Material Design under Grant No. 2019B030301001, the Science, Technology and Innovation Commission of Shenzhen Municipality (No. ZDSYS20190902092905285) and Center for Computational Science and Engineering of Southern University of Science and Technology.

References

- [1] M. S. Dresselhaus, G. Dresselhaus, and A. Jorio, *Group theory: application to the physics of condensed matter*, Springer (2008).
- [2] J. O. Dimmock, *Use of Symmetry in the Determination of Magnetic Structures*, Phys. Rev. **130**, 1337 (1963).
- [3] H. M. Rietveld, *A profile refinement method for nuclear and magnetic structures*, J. Appl. Cryst. **2**, 65 (1969).
- [4] H. Grimmer, *Comments on tables of magnetic space groups*, Acta crystallographica. Section A, Foundations of crystallography **65**, 145 (2009).
- [5] R.-J. Slager, A. Mesaros, V. Juričić, and J. Zaanen, *The space group classification of topological band-insulators*, Nat. Phys. **9**, 98 (2013).
- [6] J. Kruthoff, J. de Boer, J. van Wezel, C. L. Kane, and R.-J. Slager, *Topological Classification of Crystalline Insulators through Band Structure Combinatorics*, Phys. Rev. X **7**, 041069 (2017).
- [7] H. Watanabe, H. C. Po, and A. Vishwanath, *Structure and topology of band structures in the 1651 magnetic space groups*, Sci. Adv. **4**, eaat8685 (2018).
- [8] L. Elcoro, B. J. Wieder, Z. Song, Y. Xu, B. Bradlyn, and B. A. Bernevig, *Magnetic topological quantum chemistry*, Nat. Commun. **12**, 5965 (2021).
- [9] W. Brinkman and R. J. Elliott, *Space Group Theory for Spin Waves*, J. Appl. Phys. **37**, 1457 (1966).
- [10] W. F. Brinkman and R. J. Elliott, *Theory of spin-space groups*, Proceedings of the Royal Society of London. Series A. Mathematical and Physical Sciences **294**, 343 (1966).
- [11] D. B. Litvin and W. Opechowski, *Spin Groups*, Physica **76**, 538 (1974).
- [12] D. B. Litvin, *Spin Point Groups*, Acta. Crystallogr. A **33**, 279 (1977).
- [13] P. F. Liu, J. Y. Li, J. Z. Han, X. G. Wan, and Q. H. Liu, *Spin-Group Symmetry in Magnetic Materials with Negligible Spin-Orbit Coupling*, Phys. Rev. X **12** (2022).
- [14] A. Corticelli, R. Moessner, and P. A. McClarty, *Spin-space groups and magnon band topology*, Phys. Rev. B **105**, 064430 (2022).
- [15] L. Shekhtman, O. Entin-Wohlman, and A. Aharony, *Moriya's anisotropic superexchange interaction, frustration, and Dzyaloshinsky's weak ferromagnetism*, Phys. Rev. Lett. **69**, 836 (1992).
- [16] B. A. Bernevig, J. Orenstein, and S.-C. Zhang, *Exact SU(2) Symmetry and Persistent Spin Helix in a Spin-Orbit Coupled System*, Phys. Rev. Lett. **97**, 236601 (2006).
- [17] J. Chaloupka and G. Khaliullin, *Hidden symmetries of the extended Kitaev-Heisenberg model: Implications for the honeycomb-lattice iridates $A_2\text{IrO}_3$* , Phys. Rev. B **92**, 024413 (2015).
- [18] T. Jungwirth, X. Marti, P. Wadley, and J. Wunderlich, *Antiferromagnetic spintronics*, Nat. Nano.

11, 231 (2016).

- [19] V. Baltz, A. Manchon, M. Tsoi, T. Moriyama, T. Ono, and Y. Tserkovnyak, *Antiferromagnetic spintronics*, Rev. Mod. Phys. **90**, 015005 (2018).
- [20] L. Šmejkal, Y. Mokrousov, B. Yan, and A. H. MacDonald, *Topological antiferromagnetic spintronics*, Nat. Phys. **14**, 242 (2018).
- [21] S. Hayami, Y. Yanagi, and H. Kusunose, *Momentum-Dependent Spin Splitting by Collinear Antiferromagnetic Ordering*, J. Phys. Soc. Jpn. **88** (2019).
- [22] M. Naka, S. Hayami, H. Kusunose, Y. Yanagi, Y. Motome, and H. Seo, *Spin current generation in organic antiferromagnets*, Nat. Commun. **10**, 4305 (2019).
- [23] L. Šmejkal, R. Gonzalez-Hernandez, T. Jungwirth, and J. Sinova, *Crystal time-reversal symmetry breaking and spontaneous Hall effect in collinear antiferromagnets*, Sci. Adv. **6**, eaaz8809 (2020).
- [24] S. Hayami, Y. Yanagi, and H. Kusunose, *Bottom-up design of spin-split and reshaped electronic band structures in antiferromagnets without spin-orbit coupling: Procedure on the basis of augmented multipoles*, Phys. Rev. B **102**, 144441 (2020).
- [25] Mazin, I., K. Koepf, M. D. Johannes, R. Gonzalez-Hernandez, and L. Šmejkal, *Prediction of unconventional magnetism in doped FeSb₂*, Proc. Natl. Acad. Sci. **118** (2021).
- [26] L.-D. Yuan, Z. Wang, J.-W. Luo, and A. Zunger, *Prediction of low-Z collinear and noncollinear antiferromagnetic compounds having momentum-dependent spin splitting even without spin-orbit coupling*, Phys. Rev. Mat. **5**, 014409 (2021).
- [27] H. Y. Ma, M. Hu, N. Li, J. Liu, W. Yao, J. F. Jia, and J. Liu, *Multifunctional antiferromagnetic materials with giant piezomagnetism and noncollinear spin current*, Nat. Commun. **12**, 2846 (2021).
- [28] R. González-Hernández, L. Šmejkal, K. Výborný, Y. Yahagi, J. Sinova, T. Jungwirth, and J. Železný, *Efficient Electrical Spin Splitter Based on Nonrelativistic Collinear Antiferromagnetism*, Phys. Rev. Lett. **126**, 127701 (2021).
- [29] L. Šmejkal, J. Sinova, and T. Jungwirth, *Emerging Research Landscape of Altermagnetism*, Phys. Rev. X **12**, 040501 (2022).
- [30] L. Šmejkal, J. Sinova, and T. Jungwirth, *Beyond Conventional Ferromagnetism and Antiferromagnetism: A Phase with Nonrelativistic Spin and Crystal Rotation Symmetry*, Phys. Rev. X **12**, 031042 (2022).
- [31] S. Karube, T. Tanaka, D. Sugawara, N. Kadoguchi, M. Kohda, and J. Nitta, *Observation of Spin-Splitter Torque in Collinear Antiferromagnetic RuO₂*, Phys. Rev. Lett. **129**, 137201 (2022).
- [32] H. Bai *et al.*, *Observation of Spin Splitting Torque in a Collinear Antiferromagnet RuO₂*, Phys. Rev. Lett. **128**, 197202 (2022).
- [33] L. Šmejkal, A. B. Hellenes, R. González-Hernández, J. Sinova, and T. Jungwirth, *Giant and Tunneling Magnetoresistance in Unconventional Collinear Antiferromagnets with Nonrelativistic Spin-Momentum Coupling*, Phys. Rev. X **12**, 011028 (2022).
- [34] T. Berlijn *et al.*, *Itinerant Antiferromagnetism in RuO₂*, Phys. Rev. Lett. **118**, 077201 (2017).
- [35] A. Bose *et al.*, *Tilted spin current generated by the collinear antiferromagnet ruthenium dioxide*, Nat. Ele. **5**, 267 (2022).
- [36] Z. Feng *et al.*, *An anomalous Hall effect in altermagnetic ruthenium dioxide*, Nat. Ele. **5**, 735 (2022).
- [37] H. Bai *et al.*, *Efficient Spin-to-Charge Conversion via Altermagnetic Spin Splitting Effect in Antiferromagnet RuO₂*, Phys. Rev. Lett. **130**, 216701 (2023).

- [38] D.-F. Shao *et al.*, *Neel Spin Currents in Antiferromagnets*, Phys. Rev. Lett. **130**, 216702 (2023).
- [39] D.-F. Shao, S.-H. Zhang, M. Li, C.-B. Eom, and E. Y. Tsybal, *Spin-neutral currents for spintronics*, Nat. Commun. **12**, 7061 (2021).
- [40] Jian Yang, Zheng-Xin Liu, and C. Fang, *Symmetry invariants in magnetically ordered systems having weak spin-orbit coupling*, arXiv:2105.12738 (2021).
- [41] P.-J. Guo, Y.-W. Wei, K. Liu, Z.-X. Liu, and Z.-Y. Lu, *Eightfold Degenerate Fermions in Two Dimensions*, Phys. Rev. Lett. **127**, 176401 (2021).
- [42] P. Liu, A. Zhang, J. Han, and Q. Liu, *Chiral Dirac-like fermion in spin-orbit-free antiferromagnetic semimetals*, The Innovation **3**, 100343 (2022).
- [43] Ao Zhang *et al.*, *Chiral Dirac fermion in a collinear antiferromagnet*, arXiv:2301.12201 (2023).
- [44] L. M. Sandratskii, *Symmetry analysis of electronic states for crystals with spiral magnetic order. I. General properties*, J. Phys. Condens. Matter **3**, 8565 (1991).
- [45] C. J. Bradley and A. P. Cracknell, *The Mathematical Theory of Symmetry in Solids Representation Theory for Point Groups and Space Groups*, Oxford University Press (1972).
- [46] H. Wondratschek, in *International Tables for Crystallography Volume A1: Symmetry relations between space groups*, edited by H. Wondratschek, and U. Müller (Springer Netherlands, Dordrecht, 2004), pp. 6.
- [47] S. Ivantchev, E. Kroumova, J. Perez-Mato, J. Igarua, G. Madariaga, and H. Wondratschek, *SUPERGROUPS – a computer program for the determination of the supergroups of the space groups*, J. Appl. Cryst. **35**, 511 (2002).
- [48] L. Elcoro *et al.*, *Double crystallographic groups and their representations on the Bilbao Crystallographic Server*, J. Appl. Cryst. **50**, 1457 (2017).
- [49] E. Koch, W. Fischer, and U. Müller, in *International Tables for Crystallography, Set, Volumes A - G, OnlineMRW2016*, pp. 826.
- [50] An affine mapping is a transformation that preserve the ratios of the lengths of parallel line segments and their parallelism, but not necessarily the angles and Euclidean distances.
- [51] W. Bosma, J. Cannon, and C. Playoust, *The Magma Algebra System I: The User Language*, Journal of Symbolic Computation **24**, 235 (1997).
- [52] J. Q. Chen, M. J. Gao, and G. Q. Ma, *The Representation Group and Its Application To Space-Groups*, Rev. Mod. Phys. **57**, 211 (1985).
- [53] J.-Q. Chen, J. Ping, and F. Wang, *Group Representation Theory for Physicists* (WORLD SCIENTIFIC, 2002).
- [54] J. Yang and Z.-X. Liu, *Irreducible projective representations and their physical applications*, J. Phys. A **51**, 025207 (2017).
- [55] J. Li, Q. Yao, L. Wu, Z. Hu, B. Gao, X. Wan, and Q. Liu, *Designing light-element materials with large effective spin-orbit coupling*, Nat. Commun. **13**, 919 (2022).
- [56] D. T. Adroja *et al.*, *Muon spin rotation and neutron scattering study of the noncentrosymmetric tetragonal compound CeAuAl₃*, Phys. Rev. B **91**, 134425 (2015).
- [57] L.-D. Yuan, Z. Wang, J.-W. Luo, E. I. Rashba, and A. Zunger, *Giant momentum-dependent spin splitting in centrosymmetric low-Z antiferromagnets*, Phys. Rev. B **102**, 014422 (2020).
- [58] N. J. Ghimire, A. S. Botana, J. S. Jiang, J. Zhang, Y. S. Chen, and J. F. Mitchell, *Large anomalous Hall effect in the chiral-lattice antiferromagnet CoNb₃S₆*, Nat. Commun. **9**, 3280 (2018).
- [59] G. Tenasini *et al.*, *Giant anomalous Hall effect in quasi-two-dimensional layered antiferromagnet Co_{1/3}NbS₂*, Phys. Rev. Res **2**, 023051 (2020).

- [60] H. Tanaka *et al.*, *Large anomalous Hall effect induced by weak ferromagnetism in the noncentrosymmetric antiferromagnet CoNb_2S_6* , Phys. Rev. B **105**, L121102 (2022).
- [61] X. P. Yang *et al.*, *Visualizing the out-of-plane electronic dispersions in an intercalated transition metal dichalcogenide*, Phys. Rev. B **105**, L121107 (2022).
- [62] H. Takagi *et al.*, *Spontaneous topological Hall effect induced by non-coplanar antiferromagnetic order in intercalated van der Waals materials*, Nat. Phys. **19**, 961 (2023).
- [63] S. S. P. Parkin, E. A. Marseglia, and P. J. Brown, *Magnetic structure of $\text{Co}_{1/3}\text{NbS}_2$ and $\text{Co}_{1/3}\text{TaS}_2$* , J. Phys. C **16**, 2765 (1983).
- [64] N. Nagaosa, J. Sinova, S. Onoda, A. H. MacDonald, and N. P. Ong, *Anomalous Hall effect*, Rev. Mod. Phys. **82**, 1539 (2010).
- [65] R. Shindou and N. Nagaosa, *Orbital Ferromagnetism and Anomalous Hall Effect in Antiferromagnets on the Distorted fcc Lattice*, Phys. Rev. Lett. **87**, 116801 (2001).
- [66] M. Hirschberger *et al.*, *Geometrical Hall effect and momentum-space Berry curvature from spin-reversed band pairs*, Phys. Rev. B **103**, L041111 (2021).
- [67] L. Šmejkal, A. H. MacDonald, J. Sinova, S. Nakatsuji, and T. Jungwirth, *Anomalous Hall antiferromagnets*, Nat. Rev. Mat. **7**, 482 (2022).
- [68] Yi Jiang, Ziyin Song, Tiannian Zhu, Zhong Fang, Hongming Weng, Zheng-Xin Liu, Jian Yang, and C. Fang, *Enumeration of spin-space groups: Towards a complete description of symmetries of magnetic orders*, arXiv:2307.10371 (2023).
- [69] Zhenyu Xiao, Jianzhou Zhao, Yanqi Li, Ryuichi Shindou, and Z.-D. Song, *Spin Space Groups: Full Classification and Applications*, arXiv:2307.10364 (2023).
- [70] H. T. Stokes and D. M. Hatch, *FINDSYM: program for identifying the space-group symmetry of a crystal*, J. Appl. Cryst. **38**, 237 (2005).
- [71] I. T. Atsushi Togo, *Spglib: a software library for crystal symmetry search*, arXiv:1808.01590 (2018).
- [72] S. P. Ong *et al.*, *Python Materials Genomics (pymatgen): A robust, open-source python library for materials analysis*, Computational Materials Science **68**, 314 (2013).
- [73] G. Kresse and J. Furthmüller, *Efficient iterative schemes for ab initio total-energy calculations using a plane-wave basis set*, Phys. Rev. B **54**, 11169 (1996).
- [74] G. Kresse and D. Joubert, *From ultrasoft pseudopotentials to the projector augmented-wave method*, Phys. Rev. B **59**, 1758 (1999).
- [75] J. P. Perdew, K. Burke, and M. Ernzerhof, *Generalized Gradient Approximation Made Simple*, Phys. Rev. Lett. **77**, 3865 (1996).
- [76] S. L. Dudarev, G. A. Botton, S. Y. Savrasov, C. J. Humphreys, and A. P. Sutton, *Electron-energy-loss spectra and the structural stability of nickel oxide: An LSDA+U study*, Phys. Rev. B **57**, 1505 (1998).
- [77] A. A. Mostofi, J. R. Yates, Y.-S. Lee, I. Souza, D. Vanderbilt, and N. Marzari, *wannier90: A tool for obtaining maximally-localised Wannier functions*, Computer Physics Communications **178**, 685 (2008).
- [78] N. Marzari, A. A. Mostofi, J. R. Yates, I. Souza, and D. Vanderbilt, *Maximally localized Wannier functions: Theory and applications*, Rev. Mod. Phys. **84**, 1419 (2012).
- [79] Q. Wu, S. Zhang, H.-F. Song, M. Troyer, and A. A. Soluyanov, *WannierTools: An open-source software package for novel topological materials*, Computer Physics Communications **224**, 405 (2018).

Table I: Nontrivial SSGs for different crystal systems and different magnetic configurations. “Collinear only” indicates nontrivial SSGs that only support collinear magnetic orders, i.e., $G^S = 1$ and $\bar{1}$. Similarly, “Noncoplanar only” requires that G^S is a polyhedral PG (T , T_d , T_h , O , and O_h). “Coplanar” contains nontrivial SSGs that support coplanar magnetic orders.

Crystal system	Collinear only	Coplanar	Noncoplanar only	Total
Triclinic (2)	5	55	0	60
Monoclinic (13)	78	3540	0	3618
Orthorhombic (59)	503	53734	0	54237
Tetragonal (68)	502	31185	0	31687
Trigonal (25)	83	2331	62	2476
Hexagonal (27)	137	7149	111	7397
Cubic (36)	113	840	184	1137
Total (230)	1421	98834	357	100612

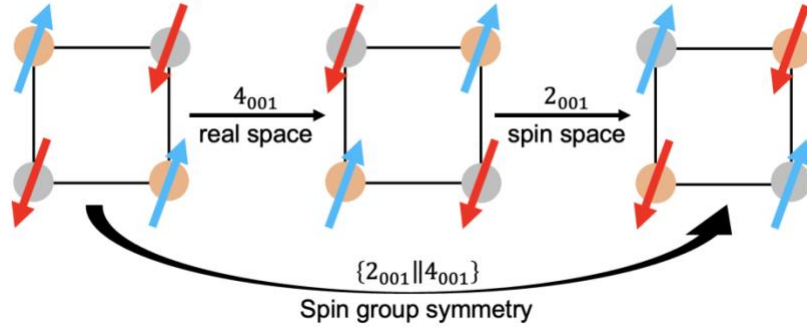


Fig. 1: Schematic plot of a spin group symmetry of an antiferromagnetic structure. It takes a four-fold rotation (4_{001}) in real space followed by a two-fold rotation (2_{001}) in spin space, constituting a spin group symmetry $\{2_{001} || 4_{001}\}$. Such a symmetry operation contains separated lattice and spin rotations, and is thus beyond the framework of magnetic groups.

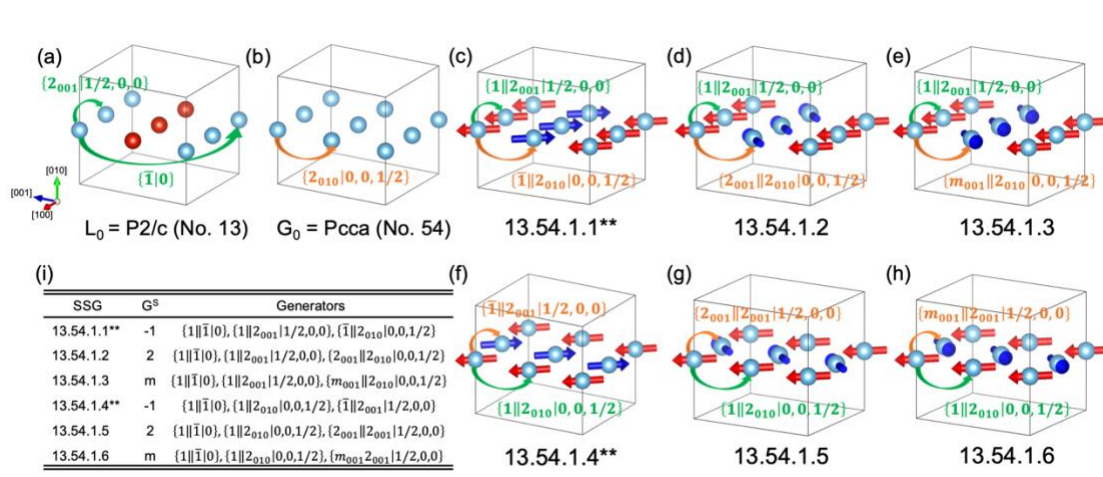


Fig. 2: SSGs generated from a t-type (L_0, G_0) subgroup pair and the corresponding magnetic configurations. (a) Structure with sublattice group $L_0 = P2/c$ (No. 13). The group generators are indicated by green arrows. The balls with different colors denote different sublattices. (b) Structure with nonmagnetic group $G_0 = Pcca$ (No. 54). The group generators that connect different sublattices are indicated by orange arrows. (c) All the generated nontrivial SSGs with their corresponding G^S and generators. (d-i) Magnetic configurations for different nontrivial SSGs. Green and orange arrows indicate the generators connecting the same and the different sublattices, respectively. Double star denotes SSGs for collinear magnetic configurations.

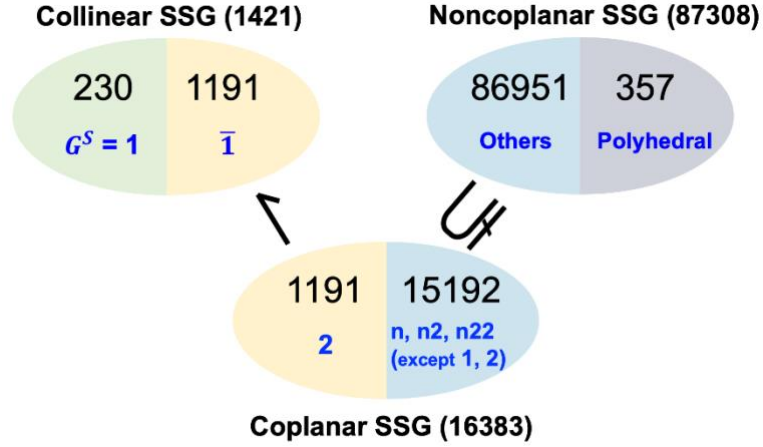


Fig. 3: Summary of inequivalent SSGs for collinear, coplanar, and noncoplanar magnetic configurations when considering their spin-only groups. The blue fonts denote the corresponding G^S . “Polyhedral” indicates polyhedral PGs, i.e., T , T_d , T_h , O , and O_h . “Others” indicates other G^S except 1, $\bar{1}$, 2, m , $2/m$, and polyhedral PGs. “ \rightarrow ” means that when considering collinear spin-only group G_{SO}^l , $G^S = \bar{1}$ and 2 yield equivalent collinear SSGs. “ \subset ” means that when considering coplanar spin-only group G_{SO}^p , the 86951 nontrivial SSGs (supporting both coplanar and noncoplanar magnetic configurations) is reduced to 15192 inequivalent coplanar SSGs.

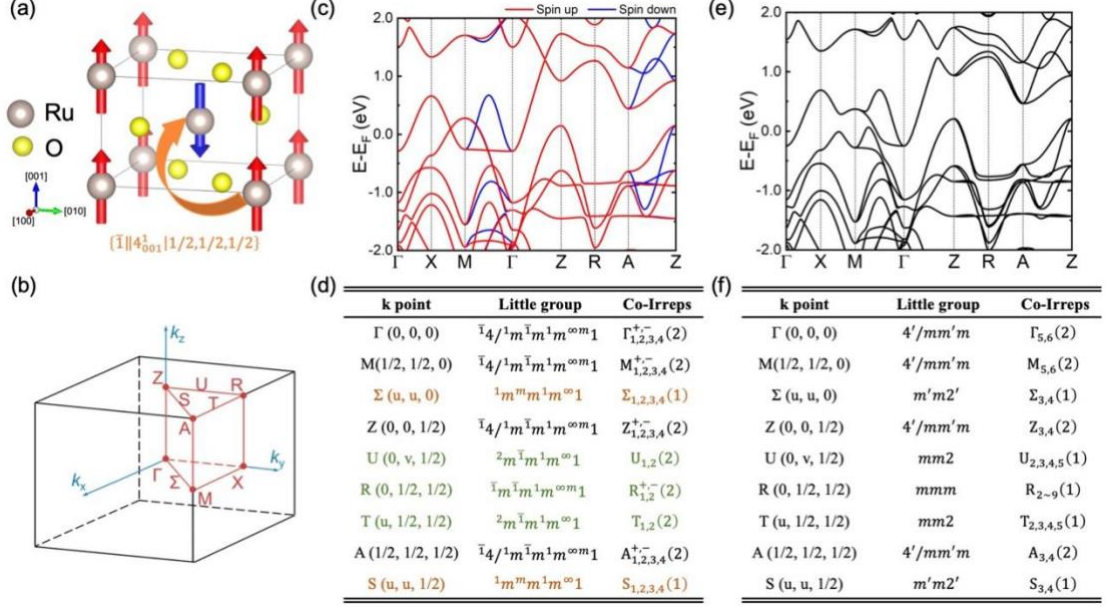


Fig. 4: Spin space group of altermagnet RuO₂. (a) Crystal structure. The symmetry connecting different sublattices are indicated. (b) Brillouin zone in momentum space. (c) SOC-free band structure with projection of the spin components. (d) Little groups and the corresponding projective co-irreps for different k -points within the regime of SSG. The notation of little group is generalized from Litvin's notation of SPGs [12]. Brown fonts denote the k -points manifesting spin splitting; Green fonts denote the k -points manifesting extra degeneracies compared with the band structure with SOC. (e) Same as (c) but with SOC. (f) Same as (d) but within the regime of MSG.

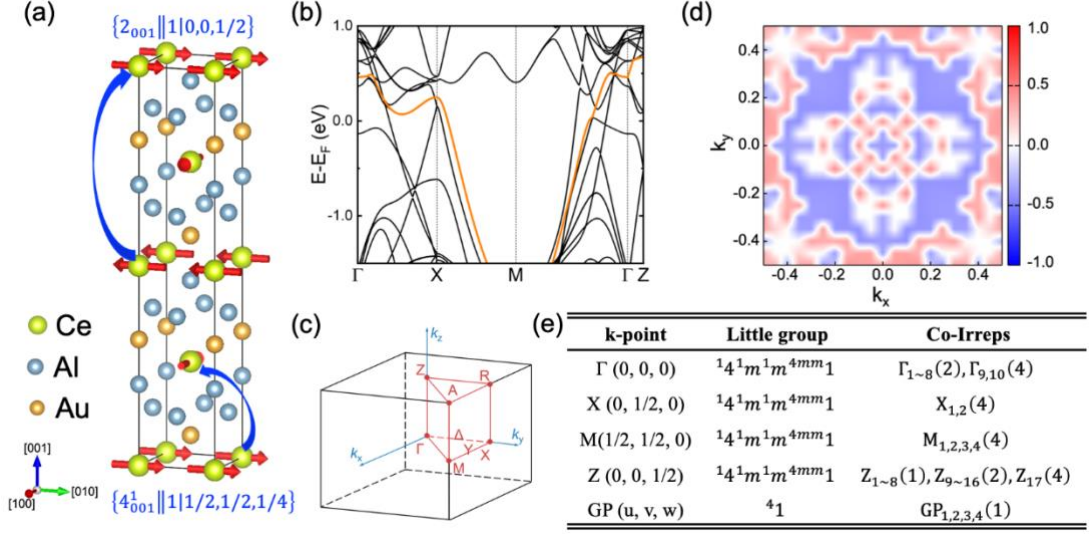


Fig. 5: Spin space group of spiral AFM CeAuAl₃. (a) Crystal structure. The symmetry connecting different sublattices are indicated. (b) Electronic band structure. (c) Brillouin zone in momentum space. (d) Spin texture at the $k_z = \pi/2$ plane for the band marked in panel (b). (e) Little groups and the corresponding projective co-irreps for different k -points. The notation of little group is generalized from Litvin's notation of SPGs [12].

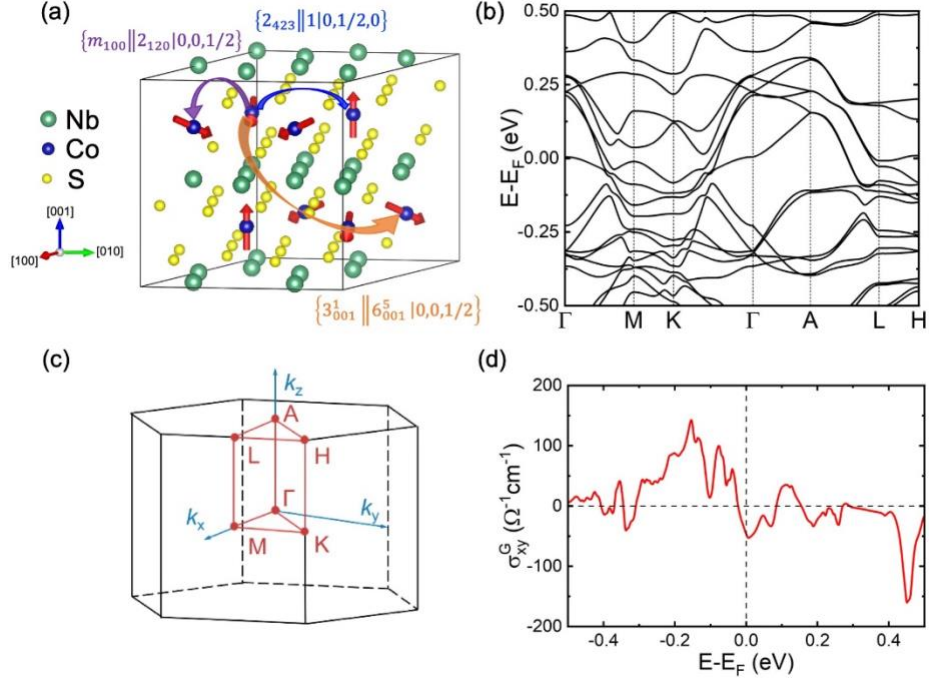


Fig. 6: Spin space group of noncoplanar AFM CoNb₃S₆. (a) Crystal structure. The symmetry connecting different sublattices are indicated. (b) Electronic band structure. (c) Brillouin zone in momentum space. (d) Geometric Hall conductivity as a function of energy. SOC is excluded in the calculations.

Appendix A: Identification of spin space group for a given magnetic structure

We develop a program to provide a convenient way to find the spin space group from a given magnetic structure (click [here](#)). The required input is a .mcif or .cif file (with magnetic moments). We recommend that the .cif file generated by FINDSYM [70] would yield more accurate results. The outputs of our program are the details of the spin space group G_{SS} , including L_0 , G_0 , i_t , i_k , G^S and all the symmetry operations, which are written based on the lattice vectors of the input structure.

The procedure of identifying the spin space group are as follows (see Fig. 6):

Step 1: Obtain the space group G of the input structure (without magnetic moment) using the module of SPGLIB [71].

Step 2: Determine whether the magnetic moments are non-coplanar, coplanar, or collinear. Extract all the magnetic moments and obtain the allowed point group for spin space using PYMATGEN [72]. Note that the magnetic moments with the same magnitude yet belonging to different orbits under G operations should be marked as inequivalent types.

Step 3: Obtain all symmetric operations of the magnetic structure. This is achieved by traversing all matches of operations of G and the spin-space point group, and applying them to the magnetic structure. The operations that keep the magnetic structure invariant form the spin space group G_{SS} .

Step 4: All elements of space operations of G_{SS} form G_0 ; all elements of G_0 that match with identity operation in spin space form the sublattice group L_0 ; all elements of spin operations of G_{SS} form point group G^S in spin space; i_k and i_t can also be obtained straightforwardly.

With all the obtained information, we can identify which spin space group the input material belongs to.

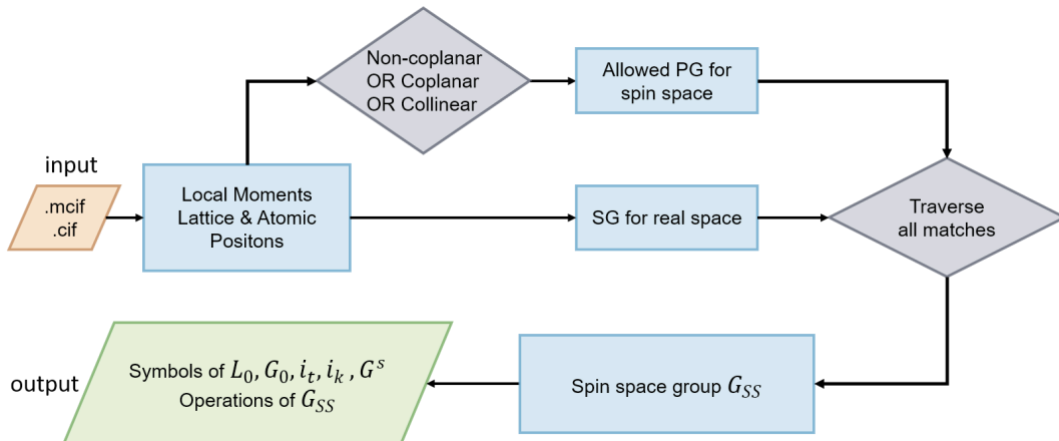


Fig. 6: Workflow of the procedure for the identification of spin space group from a given magnetic structure.

Appendix B: First-principles methods

All DFT calculations herein are performed using projector augmented wave method, implemented in Vienna ab initio simulation package (VASP) [73,74]. The generalized gradient approximation of the Perdew-Burke-Ernzerhof-type exchange-correlation potential [75] is adopted. To include the effect of electron correlation, the DFT+U approach within the rotationally invariant formalism [76] were performing with $U_{\text{eff}} = 2.0$ eV for Ru 4d (RuO_2), $U_{\text{eff}} = 4.0$ eV for Ce 4f (CeAuAl_3) and $U_{\text{eff}} = 1.0$ eV for Co 3d (CoNb_2S_6). Tight-binding models are constructed from DFT bands using the WANNIER90 package [77,78]; WannierTools package is used for the calculations of anomalous hall conductivity [79].

Appendix C: Irreducible co-representations of spiral AFM CeAuAl_3

For spiral AFM CeAuAl_3 in Fig. 5, we provide its co-irrep matrices of the generators at high-symmetry points and lines. The procedure is as follows: (1) identify the maximal unitary subgroups (MUSGs) of the little groups G_{SS}^k shown in the Fig. 5(e); (2) construct the complete set of projective irreps of MUSGs by using the CSCO approach introduced in Section III [52,54]; (3) obtain all co-irreps from those projective irreps based on the modified Dimmock and Wheeler's character sum rule, i.e., Eq. (14). Furthermore, the compatibility relation near the momentum X is also provided.

The co-irreps matrices of the SSG of CeAuAl_3 are tabulated in Tables II to VII. The corresponding compatibility relation for the momenta $\Delta(0, \nu, 0)$, $X(0, 1/2, 0)$ and $Y(u, 1/2, 0)$ (along X-M) are shown in Table VIII, which is consistent with the electronic band structure in Fig. 5(b).

Table II: Co-irrep matrices of the little group at Γ . The numbers in the parentheses in the first column denote the degree of degeneracy.

	$\{4_{001}^+ 1 1/2, 1/2,1/4\}$	$\{1 -2_{010} 0\}$	$\{1 4_{001}^+ 0\}$	$\{T2_{001} 1 0\}$
$\Gamma_1(2)$	$\begin{pmatrix} e^{\frac{\pi}{4}} & 0 \\ 0 & e^{-i\frac{\pi}{4}} \end{pmatrix}$	$\begin{pmatrix} 1 & 0 \\ 0 & 1 \end{pmatrix}$	$\begin{pmatrix} 1 & 0 \\ 0 & 1 \end{pmatrix}$	$\begin{pmatrix} 0 & 1 \\ 1 & 0 \end{pmatrix}$
$\Gamma_2(2)$	$\begin{pmatrix} e^{\frac{3\pi}{4}} & 0 \\ 0 & e^{-i\frac{3\pi}{4}} \end{pmatrix}$	$\begin{pmatrix} 1 & 0 \\ 0 & 1 \end{pmatrix}$	$\begin{pmatrix} 1 & 0 \\ 0 & 1 \end{pmatrix}$	$\begin{pmatrix} 0 & 1 \\ 1 & 0 \end{pmatrix}$
$\Gamma_3(2)$	$\begin{pmatrix} e^{-i\frac{\pi}{4}} & 0 \\ 0 & e^{\frac{\pi}{4}} \end{pmatrix}$	$\begin{pmatrix} -1 & 0 \\ 0 & -1 \end{pmatrix}$	$\begin{pmatrix} 1 & 0 \\ 0 & 1 \end{pmatrix}$	$\begin{pmatrix} 0 & 1 \\ 1 & 0 \end{pmatrix}$
$\Gamma_4(2)$	$\begin{pmatrix} e^{-i\frac{3\pi}{4}} & 0 \\ 0 & e^{\frac{3\pi}{4}} \end{pmatrix}$	$\begin{pmatrix} -1 & 0 \\ 0 & -1 \end{pmatrix}$	$\begin{pmatrix} 1 & 0 \\ 0 & 1 \end{pmatrix}$	$\begin{pmatrix} 0 & 1 \\ 1 & 0 \end{pmatrix}$
$\Gamma_5(2)$	$\begin{pmatrix} e^{-i\frac{\pi}{4}} & 0 \\ 0 & e^{\frac{\pi}{4}} \end{pmatrix}$	$\begin{pmatrix} 1 & 0 \\ 0 & 1 \end{pmatrix}$	$\begin{pmatrix} -1 & 0 \\ 0 & -1 \end{pmatrix}$	$\begin{pmatrix} 0 & 1 \\ 1 & 0 \end{pmatrix}$
$\Gamma_6(2)$	$\begin{pmatrix} e^{-i\frac{3\pi}{4}} & 0 \\ 0 & e^{\frac{3\pi}{4}} \end{pmatrix}$	$\begin{pmatrix} 1 & 0 \\ 0 & 1 \end{pmatrix}$	$\begin{pmatrix} -1 & 0 \\ 0 & -1 \end{pmatrix}$	$\begin{pmatrix} 0 & 1 \\ 1 & 0 \end{pmatrix}$
$\Gamma_7(2)$	$\begin{pmatrix} e^{\frac{3\pi}{4}} & 0 \\ 0 & e^{-i\frac{3\pi}{4}} \end{pmatrix}$	$\begin{pmatrix} -1 & 0 \\ 0 & -1 \end{pmatrix}$	$\begin{pmatrix} -1 & 0 \\ 0 & -1 \end{pmatrix}$	$\begin{pmatrix} 0 & 1 \\ 1 & 0 \end{pmatrix}$
$\Gamma_8(2)$	$\begin{pmatrix} e^{\frac{\pi}{4}} & 0 \\ 0 & e^{-i\frac{\pi}{4}} \end{pmatrix}$	$\begin{pmatrix} -1 & 0 \\ 0 & -1 \end{pmatrix}$	$\begin{pmatrix} -1 & 0 \\ 0 & -1 \end{pmatrix}$	$\begin{pmatrix} 0 & 1 \\ 1 & 0 \end{pmatrix}$
$\Gamma_9(4)$	$\begin{pmatrix} e^{-i\frac{\pi}{4}} & 0 & 0 & 0 \\ 0 & e^{-i\frac{\pi}{4}} & 0 & 0 \\ 0 & 0 & e^{i\frac{\pi}{4}} & 0 \\ 0 & 0 & 0 & e^{i\frac{\pi}{4}} \end{pmatrix}$	$\begin{pmatrix} 0 & 1 & 0 & 0 \\ 1 & 0 & 0 & 0 \\ 0 & 0 & 0 & 1 \\ 0 & 0 & 1 & 0 \end{pmatrix}$	$\begin{pmatrix} -i & 0 & 0 & 0 \\ 0 & i & 0 & 0 \\ 0 & 0 & i & 0 \\ 0 & 0 & 0 & -i \end{pmatrix}$	$\begin{pmatrix} 0 & 0 & 1 & 0 \\ 0 & 0 & 0 & 1 \\ 1 & 0 & 0 & 0 \\ 0 & 1 & 0 & 0 \end{pmatrix}$
$\Gamma_{10}(4)$	$\begin{pmatrix} e^{-i\frac{3\pi}{4}} & 0 & 0 & 0 \\ 0 & e^{-i\frac{3\pi}{4}} & 0 & 0 \\ 0 & 0 & e^{i\frac{3\pi}{4}} & 0 \\ 0 & 0 & 0 & e^{i\frac{3\pi}{4}} \end{pmatrix}$	$\begin{pmatrix} 0 & 1 & 0 & 0 \\ 1 & 0 & 0 & 0 \\ 0 & 0 & 0 & 1 \\ 0 & 0 & 1 & 0 \end{pmatrix}$	$\begin{pmatrix} -i & 0 & 0 & 0 \\ 0 & i & 0 & 0 \\ 0 & 0 & i & 0 \\ 0 & 0 & 0 & -i \end{pmatrix}$	$\begin{pmatrix} 0 & 0 & 1 & 0 \\ 0 & 0 & 0 & 1 \\ 1 & 0 & 0 & 0 \\ 0 & 1 & 0 & 0 \end{pmatrix}$

Table III: Co-irreps matrices of the little group at $\Delta(0, v, 0)$. The numbers in the parentheses in the first column denote the degree of degeneracy.

	$\{4_{001}^+ 1 1/2, 1/2,1/4\}$	$\{1 -2_{100} 0\}$	$\{T2_{001} -2_{010} 0\}$
$\Delta_1(2)$	$\begin{pmatrix} e^{-i(\frac{-\pi}{4}+v\pi)} & 0 \\ 0 & e^{-i(\frac{\pi}{4}+v\pi)} \end{pmatrix}$	$\begin{pmatrix} 1 & 0 \\ 0 & 1 \end{pmatrix}$	$\begin{pmatrix} 0 & 1 \\ 1 & 0 \end{pmatrix}$
$\Delta_2(2)$	$\begin{pmatrix} e^{-i(\frac{-3\pi}{4}+v\pi)} & 0 \\ 0 & e^{-i(\frac{3\pi}{4}+v\pi)} \end{pmatrix}$	$\begin{pmatrix} 1 & 0 \\ 0 & 1 \end{pmatrix}$	$\begin{pmatrix} 0 & 1 \\ 1 & 0 \end{pmatrix}$
$\Delta_3(2)$	$\begin{pmatrix} e^{-i(\frac{\pi}{4}+v\pi)} & 0 \\ 0 & e^{-i(\frac{-\pi}{4}+v\pi)} \end{pmatrix}$	$\begin{pmatrix} -1 & 0 \\ 0 & -1 \end{pmatrix}$	$\begin{pmatrix} 0 & 1 \\ 1 & 0 \end{pmatrix}$
$\Delta_4(2)$	$\begin{pmatrix} e^{-i(\frac{3\pi}{4}+v\pi)} & 0 \\ 0 & e^{-i(\frac{-3\pi}{4}+v\pi)} \end{pmatrix}$	$\begin{pmatrix} -1 & 0 \\ 0 & -1 \end{pmatrix}$	$\begin{pmatrix} 0 & 1 \\ 1 & 0 \end{pmatrix}$

Table IV: Co-irreps matrices of the little group at X. The numbers in the parentheses in the first column denote the degree of degeneracy.

	$\{4_{001}^+ 1 1/2, 1/2,1/4\}$	$\{1 -2_{010} 0\}$	$\{1 2_{001} 0\}$	$\{T2_{001} 1 0\}$
$X_1(4)$	$\begin{pmatrix} 0 & i & 0 & 0 \\ -1 & 0 & 0 & 0 \\ 0 & 0 & 0 & -i \\ 0 & 0 & -1 & 0 \end{pmatrix}$	$\begin{pmatrix} 1 & 0 & 0 & 0 \\ 0 & -1 & 0 & 0 \\ 0 & 0 & 1 & 0 \\ 0 & 0 & 0 & -1 \end{pmatrix}$	$\begin{pmatrix} 1 & 0 & 0 & 0 \\ 0 & -1 & 0 & 0 \\ 0 & 0 & 1 & 0 \\ 0 & 0 & 0 & -1 \end{pmatrix}$	$\begin{pmatrix} 0 & 0 & 1 & 0 \\ 0 & 0 & 0 & 1 \\ 1 & 0 & 0 & 0 \\ 0 & 1 & 0 & 0 \end{pmatrix}$
$X_2(4)$	$\begin{pmatrix} 0 & -i & 0 & 0 \\ -1 & 0 & 0 & 0 \\ 0 & 0 & 0 & i \\ 0 & 0 & -1 & 0 \end{pmatrix}$	$\begin{pmatrix} 1 & 0 & 0 & 0 \\ 0 & -1 & 0 & 0 \\ 0 & 0 & 1 & 0 \\ 0 & 0 & 0 & -1 \end{pmatrix}$	$\begin{pmatrix} -1 & 0 & 0 & 0 \\ 0 & 1 & 0 & 0 \\ 0 & 0 & -1 & 0 \\ 0 & 0 & 0 & 1 \end{pmatrix}$	$\begin{pmatrix} 0 & 0 & 1 & 0 \\ 0 & 0 & 0 & 1 \\ 1 & 0 & 0 & 0 \\ 0 & 1 & 0 & 0 \end{pmatrix}$

Table V: Co-irreps matrices of the little group at Y(u,1/2,0). The numbers in the parentheses in the first column denote the degree of degeneracy.

	$\{4_{001}^+ 1 1/2,1/2,1/4\}$	$\{1 -2_{010} 0\}$	$\{T2_{001} -2_{100} 0\}$
$Y_1(4)$	$\begin{pmatrix} e^{-i(\frac{5\pi}{4}+u\pi)} & 0 & 0 & 0 \\ 0 & e^{-i(\frac{\pi}{4}+u\pi)} & 0 & 0 \\ 0 & 0 & e^{-i(\frac{3\pi}{4}+u\pi)} & 0 \\ 0 & 0 & 0 & e^{-i(\frac{7\pi}{4}+u\pi)} \end{pmatrix}$	$\begin{pmatrix} 0 & e^{\frac{3\pi}{4}} & 0 & 0 \\ e^{-i\frac{3\pi}{4}} & 0 & 0 & 0 \\ 0 & 0 & 0 & e^{-i\frac{3\pi}{4}} \\ 0 & 0 & e^{\frac{3\pi}{4}} & 0 \end{pmatrix}$	$\begin{pmatrix} 0 & 0 & 1 & 0 \\ 0 & 0 & 0 & 1 \\ 1 & 0 & 0 & 0 \\ 0 & 1 & 0 & 0 \end{pmatrix}$

Table VI: Co-irreps matrices of the little group at M. The numbers in the parentheses in the first column denote the degree of degeneracy.

	$\{4_{001}^+ 1 1/2, 1/2,1/4\}$	$\{1 -2_{010} 0\}$	$\{1 4_{001}^+ 0\}$	$\{T2_{001} 1 0\}$
$M_1(4)$	$\begin{pmatrix} 0 & 1 & 0 & 0 \\ i & 0 & 0 & 0 \\ 0 & 0 & 0 & 1 \\ 0 & 0 & -i & 0 \end{pmatrix}$	$\begin{pmatrix} 1 & 0 & 0 & 0 \\ 0 & -1 & 0 & 0 \\ 0 & 0 & 1 & 0 \\ 0 & 0 & 0 & -1 \end{pmatrix}$	$\begin{pmatrix} 1 & 0 & 0 & 0 \\ 0 & -1 & 0 & 0 \\ 0 & 0 & 1 & 0 \\ 0 & 0 & 0 & -1 \end{pmatrix}$	$\begin{pmatrix} 0 & 0 & 1 & 0 \\ 0 & 0 & 0 & 1 \\ 1 & 0 & 0 & 0 \\ 0 & 1 & 0 & 0 \end{pmatrix}$
$M_2(4)$	$\begin{pmatrix} 0 & i & 0 & 0 \\ -1 & 0 & 0 & 0 \\ 0 & 0 & 0 & -i \\ 0 & 0 & -1 & 0 \end{pmatrix}$	$\begin{pmatrix} 1 & 0 & 0 & 0 \\ 0 & -1 & 0 & 0 \\ 0 & 0 & 1 & 0 \\ 0 & 0 & 0 & -1 \end{pmatrix}$	$\begin{pmatrix} -1 & 0 & 0 & 0 \\ 0 & 1 & 0 & 0 \\ 0 & 0 & -1 & 0 \\ 0 & 0 & 0 & 1 \end{pmatrix}$	$\begin{pmatrix} 0 & 0 & 1 & 0 \\ 0 & 0 & 0 & 1 \\ 1 & 0 & 0 & 0 \\ 0 & 1 & 0 & 0 \end{pmatrix}$
$M_3(4)$	$\begin{pmatrix} 0 & i & 0 & 0 \\ -1 & 0 & 0 & 0 \\ 0 & 0 & 0 & -i \\ 0 & 0 & -1 & 0 \end{pmatrix}$	$\begin{pmatrix} 0 & e^{-i\frac{3\pi}{4}} & 0 & 0 \\ e^{i\frac{3\pi}{4}} & 0 & 0 & 0 \\ 0 & 0 & 0 & e^{i\frac{3\pi}{4}} \\ 0 & 0 & e^{-i\frac{3\pi}{4}} & 0 \end{pmatrix}$	$\begin{pmatrix} -1 & 0 & 0 & 0 \\ 0 & 1 & 0 & 0 \\ 0 & 0 & 1 & 0 \\ 0 & 0 & 0 & -1 \end{pmatrix}$	$\begin{pmatrix} 0 & 0 & 1 & 0 \\ 0 & 0 & 0 & 1 \\ 1 & 0 & 0 & 0 \\ 0 & 1 & 0 & 0 \end{pmatrix}$
$M_4(4)$	$\begin{pmatrix} 0 & e^{i\frac{\pi}{4}} & 0 & 0 \\ e^{i\frac{\pi}{4}} & 0 & 0 & 0 \\ 0 & 0 & 0 & e^{-i\frac{\pi}{4}} \\ 0 & 0 & e^{-i\frac{\pi}{4}} & 0 \end{pmatrix}$	$\begin{pmatrix} 0 & -i & 0 & 0 \\ i & 0 & 0 & 0 \\ 0 & 0 & 0 & i \\ 0 & 0 & -i & 0 \end{pmatrix}$	$\begin{pmatrix} -i & 0 & 0 & 0 \\ 0 & i & 0 & 0 \\ 0 & 0 & i & 0 \\ 0 & 0 & 0 & -i \end{pmatrix}$	$\begin{pmatrix} 0 & 0 & 1 & 0 \\ 0 & 0 & 0 & 1 \\ 1 & 0 & 0 & 0 \\ 0 & 1 & 0 & 0 \end{pmatrix}$

Table VII: Co-irreps matrices of the little group at Z. The numbers in the parentheses

in the first column denote the degree of degeneracy.

	$\{4_{001}^+ 1 1/2, 1/2,1/4\}$	$\{1 -2_{010} 0\}$	$\{1 4_{001}^+ 0\}$	$\{T2_{001} 1 0\}$
$Z_1(1)$	1	1	1	1
$Z_2(1)$	-1	1	1	1
$Z_3(1)$	1	-1	1	1
$Z_4(1)$	-1	-1	1	1
$Z_5(1)$	1	1	-1	1
$Z_6(1)$	-1	1	-1	1
$Z_7(1)$	-1	-1	-1	1
$Z_8(1)$	1	-1	-1	1
$Z_9(2)$	$\begin{pmatrix} -i & 0 \\ 0 & i \end{pmatrix}$	$\begin{pmatrix} 1 & 0 \\ 0 & 1 \end{pmatrix}$	$\begin{pmatrix} 1 & 0 \\ 0 & 1 \end{pmatrix}$	$\begin{pmatrix} 0 & 1 \\ 1 & 0 \end{pmatrix}$
$Z_{10}(2)$	$\begin{pmatrix} -i & 0 \\ 0 & i \end{pmatrix}$	$\begin{pmatrix} -1 & 0 \\ 0 & -1 \end{pmatrix}$	$\begin{pmatrix} 1 & 0 \\ 0 & 1 \end{pmatrix}$	$\begin{pmatrix} 0 & 1 \\ 1 & 0 \end{pmatrix}$
$Z_{11}(2)$	$\begin{pmatrix} -i & 0 \\ 0 & i \end{pmatrix}$	$\begin{pmatrix} 1 & 0 \\ 0 & 1 \end{pmatrix}$	$\begin{pmatrix} -1 & 0 \\ 0 & -1 \end{pmatrix}$	$\begin{pmatrix} 0 & 1 \\ 1 & 0 \end{pmatrix}$
$Z_{12}(2)$	$\begin{pmatrix} i & 0 \\ 0 & -i \end{pmatrix}$	$\begin{pmatrix} -1 & 0 \\ 0 & -1 \end{pmatrix}$	$\begin{pmatrix} -1 & 0 \\ 0 & -1 \end{pmatrix}$	$\begin{pmatrix} 0 & 1 \\ 1 & 0 \end{pmatrix}$
$Z_{13}(2)$	$\begin{pmatrix} 1 & 0 \\ 0 & 1 \end{pmatrix}$	$\begin{pmatrix} 0 & 1 \\ 1 & 0 \end{pmatrix}$	$\begin{pmatrix} i & 0 \\ 0 & -i \end{pmatrix}$	$\begin{pmatrix} 0 & 1 \\ 1 & 0 \end{pmatrix}$
$Z_{14}(2)$	$\begin{pmatrix} -1 & 0 \\ 0 & -1 \end{pmatrix}$	$\begin{pmatrix} 0 & 1 \\ 1 & 0 \end{pmatrix}$	$\begin{pmatrix} -i & 0 \\ 0 & i \end{pmatrix}$	$\begin{pmatrix} 0 & 1 \\ 1 & 0 \end{pmatrix}$
$Z_{15}(2)$	$\begin{pmatrix} 1 & 0 \\ 0 & 1 \end{pmatrix}$	$\begin{pmatrix} 0 & -1 \\ -1 & 0 \end{pmatrix}$	$\begin{pmatrix} -i & 0 \\ 0 & i \end{pmatrix}$	$\begin{pmatrix} 0 & 1 \\ 1 & 0 \end{pmatrix}$
$Z_{16}(2)$	$\begin{pmatrix} -1 & 0 \\ 0 & -1 \end{pmatrix}$	$\begin{pmatrix} 0 & e^{\frac{3\pi}{4}} \\ e^{-\frac{3\pi}{4}} & 0 \end{pmatrix}$	$\begin{pmatrix} i & 0 \\ 0 & -i \end{pmatrix}$	$\begin{pmatrix} 0 & 1 \\ 1 & 0 \end{pmatrix}$
$Z_{17}(4)$	$\begin{pmatrix} -i & 0 & 0 & 0 \\ 0 & -i & 0 & 0 \\ 0 & 0 & i & 0 \\ 0 & 0 & 0 & i \end{pmatrix}$	$\begin{pmatrix} 0 & 1 & 0 & 0 \\ 1 & 0 & 0 & 0 \\ 0 & 0 & 0 & 1 \\ 0 & 0 & 1 & 0 \end{pmatrix}$	$\begin{pmatrix} -i & 0 & 0 & 0 \\ 0 & i & 0 & 0 \\ 0 & 0 & i & 0 \\ 0 & 0 & 0 & -i \end{pmatrix}$	$\begin{pmatrix} 0 & 0 & 1 & 0 \\ 0 & 0 & 0 & 1 \\ 1 & 0 & 0 & 0 \\ 0 & 1 & 0 & 0 \end{pmatrix}$

Table VIII: Compatibility relation for Δ , X and Y. The second row shows the little groups for the corresponding momenta.

Δ	X	Y
$^1m_{100} \ ^4mm1$	$^14^1m^1m^4mm1$	$^1m_{010} \ ^4mm1$
$\Delta_1(2) \oplus \Delta_2(2)$	$X_1(4)$	$Y_1(4)$
$\Delta_3(2) \oplus \Delta_4(2)$	$X_2(4)$	$Y_1(4)$

Supplementary Materials

Enumeration and representation of spin space groups

Jun Ren^{1,†}, Xiaobing Chen^{1,†}, Yanzhou Zhu^{2,†}, Yutong Yu¹, Ao Zhang¹,
Jiayu Li¹, Yuntian Liu¹, Caiheng Li² and Qihang Liu^{1,3,4,*}

¹*Shenzhen Institute for Quantum Science and Engineering and Department of Physics,
Southern University of Science and Technology, Shenzhen 518055, China*

²*National Center for Applied Mathematics Shenzhen, and Department of Mathematics,
Southern University of Science and Technology, Shenzhen 518055, China*

³*Guangdong Provincial Key Laboratory of Computational Science and Material
Design, Southern University of Science and Technology, Shenzhen 518055, China*

⁴*Shenzhen Key Laboratory of Advanced Quantum Functional Materials and Devices,
Southern University of Science and Technology, Shenzhen 518055, China*

[†]These authors contributed equally to this work.

*Email: liuqh@sustech.edu.cn

This material contains the full list of the nontrivial spin space groups G_{NS} , including their four-segment identification (G_0, L_0, i_k, m) , transformation matrices M_T , coupled point groups in spin space G^s , and generators of quotient group G_0/L_0 . For the full list please click [here](#).